

# UNCLASSIFIED

AD NUMBER	
AD140228	
CLASSIFICATION CHANGES	
TO:	unclassified
FROM:	confidential
LIMITATION CHANGES	
TO:	Approved for public release, distribution unlimited
FROM:	Distribution authorized to U.S. Gov't. agencies and their contractors; Administrative/Operational Use; 11 JUL 1956. Other requests shall be referred to Office of Naval Research, Suite 1425, 875 North Randolph Street, Arlington, VA 22203-1995.
AUTHORITY	
ONR ltr dtd 28 Jul 1977; ONR ltr dtd 28 Jul 1977	

THIS PAGE IS UNCLASSIFIED

THIS REPORT HAS BEEN DELIMITED  
AND CLEARED FOR PUBLIC RELEASE  
UNDER DOD DIRECTIVE 5200.20 AND  
NO RESTRICTIONS ARE IMPOSED UPON  
ITS USE AND DISCLOSURE.

DISTRIBUTION STATEMENT A

APPROVED FOR PUBLIC RELEASE;  
DISTRIBUTION UNLIMITED.

**UNCLASSIFIED**

**AD 140228**

**DEFENSE DOCUMENTATION CENTER**

**FOR**

**SCIENTIFIC AND TECHNICAL INFORMATION**

**CAMERON STATION ALEXANDRIA VIRGINIA**

**CLASSIFICATION CHANGED**

**TO UNCLASSIFIED**

**FROM CONFIDENTIAL**

**PER AUTHORITY LISTED IN**

**DDC TAB NO. U4-8 P800. 148**

**DATE 15 APR. 64**



**UNCLASSIFIED**

NOTICE: When government or other drawings, specifications or other data are used for any purpose other than in connection with a definitely related government procurement operation, the U. S. Government thereby incurs no responsibility, nor any obligation whatsoever; and the fact that the Government may have formulated, furnished, or in any way supplied the said drawings, specifications, or other data is not to be regarded by implication or otherwise as in any manner licensing the holder or any other person or corporation, or conveying any rights or permission to manufacture, use or sell any patented invention that may in any way be related thereto.

CONFIDENTIAL

**FC**

**VTOL TRANSPORT AIRCRAFT**

# Comparative Study

**PROPELLER AERODYNAMICS  
VERTOL REPORT NO. R-77**

SEP 9 1957

**VERTOL**

**7AA 42113**

*Aircraft Corporation*

*formerly Piasecki Helicopter Corporation*

CONFIDENTIAL

**This document is the property of the United States Government. It is furnished for the duration of the contract and shall be returned when no longer required, or upon recall by ASTIA to the following address:  
Armed Services Technical Information Agency, Document Service Center,  
Knott Building, Dayton 2, Ohio.**

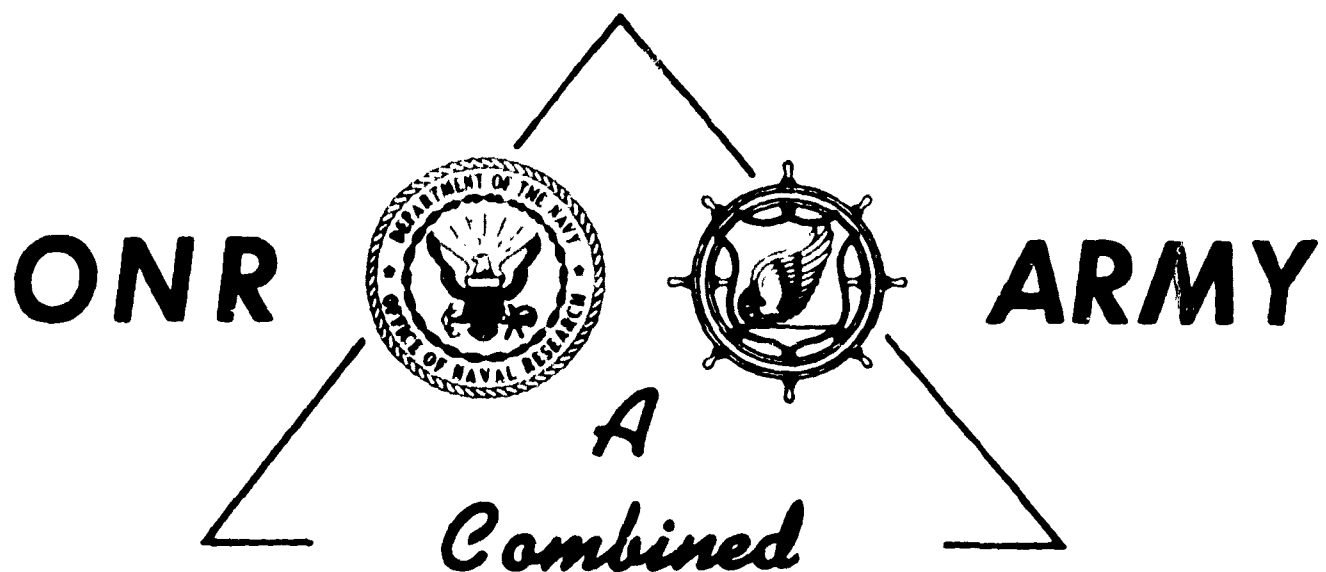
**NOTICE: THIS DOCUMENT CONTAINS INFORMATION AFFECTING THE NATIONAL DEFENSE OF THE UNITED STATES WITHIN THE MEANING OF THE ESPIONAGE LAWS, TITLE 18, U.S.C., SECTIONS 793 and 794. THE TRANSMISSION OR THE REVELATION OF ITS CONTENTS IN ANY MANNER TO AN UNAUTHORIZED PERSON IS PROHIBITED BY LA**

CONFIDENTIAL

# Comparative Study of Various Types of **VTOL Transport Aircraft**

## PROPELLER AERODYNAMICS REPORT R-77

Vertol Aircraft Corporation      Morton, Pennsylvania



### Research and Development Program

### Contract NON 1681(00)

This document contains information affecting the national defense of the United States within the meaning of the Espionage Laws, Title 18, U.S.C., Sections 793 and 794. The transmission or the revelation of its contents in any manner to an unauthorized person is prohibited by law.

Reproduction in whole or in part is permitted for any purpose of the United States Government.

PREPARED BY  
**B. W. McCORMICK, JR.**

Supervised by *W. Z. Stepniewski*  
**W. Z. STEPNIEWSKI** Chief - R&D

Approved by *L. L. Douglas*  
**L. L. DOUGLAS** Vice Pres. - Engineering

**71A 42113**

Copy No. 4

CONFIDENTIAL

JULY 13, 1956

TABLE OF CONTENTS

	<u>Page</u>
Figures	11
I. Summary	1
II. Notation	2
III. Introduction	4
IV. Development of Theory	
A. The Optimum Rotor for Hovering	6
B. Application of Equations to Design of Rotor	10
C. Selection of Optimum Rotor Parameters	11
D. The Optimum Propeller	16
E. Selection of Optimum Propeller Parameters	18
F. Comparison of Optimum Rotor with the Optimum Propeller	21
G. Analysis of Given Rotor or Propeller	22
H. Results of Digital Computer Program	25
V. Conclusions	29
VI. References	32
Figures	34-53



FIGURES

1. Rotor Blade Element in Hovering
2. Relationship between Optimum Solidity, Thrust Coefficient and Average Lift Coefficient for a Rotor
3. Optimum Efficiency
4. Propeller Blade Element
5. Relationship between Optimum Solidity, Thrust Coefficient and  $\lambda$  for a Propeller
6. Calculated Performance of Constant-Pitch Rotors
7. Effect of Mach Number on the Performance of Constant-Pitch Rotors
8. Calculated Performance of Constant-Pitch Rotors with  $C_{l_{avg}} = 0.5$  Acting as Propellers
9. Calculated Performance of Constant-Pitch Rotors with  $C_{l_{avg}} = 0.5$  Acting as Propellers
10. Calculated Performance of Constant-Pitch Rotors with  $C_{l_{avg}} = 0.5$  Acting as Propellers
11. Calculated Performance of Constant-Pitch Propellers
12. Calculated Performance of Constant-Pitch Propellers
13. Calculated Performance of Constant-Pitch Propellers

14. Calculated Performance of Constant-Pitch Propellers with  $C_T = .005$   
Acting as Rotors ( $\lambda = 0.5$ )
15. Calculated Performance of Constant-Pitch Propellers with  $C_T = .005$   
Acting as Rotors ( $\lambda = 0.6$ )
16. Calculated Performance of Constant-Pitch Propellers with  $C_T = .005$   
Acting as Rotors ( $\lambda = 0.7$ )
17. Comparison of Power Required by an Optimum Rotor and an Optimum  
Propeller with Both Performing as a Propeller
18. Comparison of Power Required by an Optimum Rotor and an Optimum  
Propeller with Both Performing as a Rotor
19. Power Required by Optimum Rotor and Optimum Propeller to Hover  
Example Tilt-Wing Transport
20. Power Required by Optimum Rotor and Optimum Propeller to Propel  
the Example Tilt-Wing Transport in Forward Flight

**I. SUMMARY**

The vortex theory of propellers is developed in a manner suitable for the analysis of propellers for tilt-wing VTOL aircraft. Expressions defining the optimum rotor and the optimum propeller are developed. However, it is shown that a single design cannot be made which will satisfy simultaneously both optimums. From the results of computations performed with an automatic digital computer, it is concluded that in order to obtain good performance from a single design acting as both a rotor and a propeller, the propeller should be designed to operate at a high advance ratio in the airplane state. In addition, depending upon the blade solidity, the design of the propeller, with regard to pitch distribution and planform, should favor operation as a propeller rather than as a rotor.

II. NOTATION

a	$b/\sqrt{2 C_T}$
$a_0$	$d C_l / d \alpha$
$a_{0inc}$	$a_0$ for incompressible flow
b	number of blades
c	section chord
$C_d$	section drag coefficient
$C_l$	section lift coefficient
$C_{lavg}$	average lift coefficient
$C_p$	power coefficient = $P/\rho V_T^3 \pi R^2$
$C_t$	thrust coefficient = $T/\rho V_T^2 \pi R^2$
D	propeller diameter
F	averaging factor for induced velocity
$F_Q$	torque force
k	blade taper
M	figure of merit; also, Mach number
$M_{cr}$	critical Mach number
p	blade pitch
P	power
$P_i$	induced power
$P_p$	profile power
r	station radius
$r_h$	hub radius
R	propeller radius
T	thrust
V	advance velocity

$V_e$	resultant velocity (see Figure 4)
$V_r$	resultant velocity (see Figure 4)
$V_t$	tip velocity due to rotation only
$w$	propeller induced velocity
$w_a$	axial component of $w$
$w_t$	tangential component of $w$
$w_o$	impact velocity (see Figure 4)
$w_o'$	$w_o/V_T$
$x$	$r/R$
$x_h$	$r_h/R$
$\alpha$	angle of attack
$\alpha_i$	induced angle of attack
$\beta$	blade pitch angle
$\Delta\beta$	change in
$\sigma$	$C_{T_{opt}}/C_T$
$\Gamma$	bound circulation
$\epsilon$	$C_d/C_l$
$\omega$	angular velocity
$\phi$	resultant flow angle
$\phi_T$	$\phi$ for $X = 1$
$\sigma$	solidity = $bc/\pi r$
$\sigma_o$	solidity for $X = 0$
$\eta$	propeller efficiency = $C_T \lambda / C_p$
$\eta_o$	design efficiency for rotor
$\lambda$	$V/V_T$

subscript "opt" denotes optimum

### III. INTRODUCTION

There are many factors to be considered in the design of rotors for VTOL aircraft. This present study is limited to the aerodynamic considerations.

It is fundamental that any device designed to perform a number of functions is usually never as efficient in performing any given one of those functions as a device designed specifically for that particular function. Similarly, it is to be expected that a rotor for a VTOL aircraft will not be as efficient a rotor as a helicopter rotor or as efficient of a propeller as an airplane propeller. The main difficulty in the design of a VTOL rotor is the fact that as a rotor it is loaded relatively heavy, while as a propeller it is lightly loaded. A compromise must be reached between these two states of operation.

There are several approaches which can be taken to this problem. First, the optimum designs as a rotor and as a propeller can both be investigated to determine the differences between the two. Next, the optimum rotor can be analyzed as a propeller and inversely the optimum propeller can be analyzed as a rotor. Finally, arbitrary designs can be analyzed as both a rotor and a propeller.

Other artificial means, such as retractable blades, boundary layer control or a blade with the ability to vary its twist are possible answers to satisfying the two regimes of operation. However, these are beyond the scope of this presentation.

CONFIDENTIAL

Page 5  
Report R-77

In this development, the following problems are considered. First, the optimum twist is calculated for a rotor in hovering having a given planform and tip speed. This is then followed by the general investigation of the optimum combination of blade parameters for a rotor. These same analyses are then performed for a propeller. Finally, the analysis of a given rotor or propeller is made.

It will be seen that the optimum combination of blade parameters for a rotor and a propeller are appreciably different. In view of this conclusion, attention was given more to the analysis of constant pitch rotors performing as both rotors and propellers. A program was set up on a digital computer to study the effects of varying pertinent blade parameters. The results of these calculations are presented and discussed in the conclusions of this study.

It should be emphasized, and the reader cautioned to the fact, that this report is not intended to be a VTOL propeller design handbook. Its intended purpose is to investigate, in a broad sense, the relative merits of different design philosophies of propellers for tilt-wing, VTOL aircraft. The calculated performances presented here in comparison with measured results will probably prove somewhat optimistic. This is due to the fact a very clean airfoil section is assumed in the calculations and, in addition, the effect of a hub is ignored with all numerical integrations being carried into the axis of rotation.

CONFIDENTIAL

IV. DEVELOPMENT OF THEORYA. The Optimum Rotor for Hovering

The following development is based on the vortex theory of propellers as presented in references (1) and (2). A blade element in hovering is shown in Figure 1. In this figure the following quantities are defined as:

- $\Gamma$  = bound circulation
- $F_Q$  = torque force
- $T$  = thrust
- $w$  = induced velocity
- $w_a$  = axial component of  $w$
- $w_t$  = tangential component of  $w$
- $w_0$  = fictitious "impact" velocity
- $V_e$  = resultant velocity
- $r$  = section radius
- $x$  =  $r/R$
- $R$  = rotor radius
- $V_t$  = tip velocity due to rotation

The Betz condition for the optimum propeller is well known and states that the impact velocity,  $w_0$ , must be a constant for minimum induced power loss. In addition to this condition, the induced velocity,  $w$ , must be approximately normal to the resultant velocity  $V_e$ . This condition of normality can be shown to hold exactly only in the ultimate wake where the induced velocity has increased to twice its value at the plane of the rotor.



From the geometry of Figure 1, it follows that:

$$\tan \phi = \frac{w_o}{\lambda V_T} = \frac{w_a}{\lambda V_T - w_t} = \frac{w_t}{w_a} = \frac{w_o'}{\lambda} \quad (1)$$

$$w_a = w_o \cos^2 \phi \quad (b)$$

$$w_t = w_o \cos \phi \sin \phi \quad (c)$$

$$V_o = \lambda V_T \cos \phi \quad (d)$$

$$\text{where: } w_o' = \frac{w_o}{V_T}$$

the Kutta-Joukowski law states that:

$$F = \rho \bar{V} \times \bar{\Gamma} \quad (2)$$

thus, if  $b$  is the number of blades:

$$dT = b \rho (\lambda V_T - w_t) \Gamma \quad (a)$$

$$dF_Q = b \rho w_a \Gamma dr \quad (b)$$

The circulation  $\Gamma$  and the tangential component of induced velocity can be related by a factor,  $F$ .

$$b \Gamma = 4\pi r F w_t \quad (3)$$

The factor,  $F$ , has been calculated approximately by Prandtl to be:

$$F = \frac{2}{\pi} \cos^2 \phi_T \exp \left[ \frac{-b(1-\lambda)}{2 \sin \phi_T} \right] \quad (4)$$

$$\text{where: } \phi_T = \phi \text{ at } \lambda = 1$$

Although this is an approximation to the more exact Goldstein's factor, it should agree closely with Goldstein's factor for rotors.

If equations (1) and (3) are substituted into (2) then the thrust and power coefficients can be calculated as:

$$C_T = 4 \omega_o'^2 \int_{x_h}^1 F x \cos^4 \phi dx \quad (a) \quad (5)$$

$$C_p = 4 \omega_o'^3 \int_{x_h}^1 F x \cos^4 \phi dx \quad (b)$$

where:  $C_T = T / \rho \pi R^2 V_T^2$   
 $C_p = P / \rho \pi R^2 V_T^3$   
 $P = \text{power}$   
 $x_h = \text{hub radius}/R$

Equations (5 a and b) neglect any profile drag losses. If these are included, then the thrust and power coefficients become:

$$C_T = 4 \omega_o'^2 \int_{x_h}^1 F x \cos^4 \phi (1 - \epsilon \tan \phi) dx \quad (a) \quad (6)$$

$$C_p = 4 \omega_o'^3 \int_{x_h}^1 F x \cos^4 \phi (1 + \epsilon \cot \phi) dx \quad (b)$$

where:  $\epsilon = C_d / C_l$   
 $C_d = \text{profile drag coefficient}$   
 $C_l = \text{section lift coefficient}$

It is often convenient to consider a rotor in terms of an average lift coefficient. This can be calculated by ignoring the induced velocity in calculating the thrust.

$$\begin{aligned} T &= \frac{b}{2} \rho \int_{r_h}^R (x V_T)^2 c C_l dr \\ &= \frac{b}{2} \rho C_{l_{avg}} \int_{r_h}^R (x V_T)^2 c dr \end{aligned} \quad (7)$$

or

$$C_{l_{avg}} = \frac{\int_{x_h}^1 x^2 \frac{c}{R} dx}{\int_{x_h}^1 x^2 \frac{c}{R} dx}$$

where:  $c$  = section chord

This can also be written in terms of the thrust coefficient.

$$C_{l_{avg}} = \frac{2\pi C_T}{b \int_{x_h}^1 x^2 \frac{c}{R} dx} \quad (8)$$

For a uniformly tapered blade where the chord is given by:

$$\frac{c}{R} = \frac{c_o}{R} (1 - kx)$$

the average lift coefficient becomes:

$$C_{l_{avg}} = \frac{6 C_T}{\sigma_o f(x_h, k)} \quad (9)$$

where:  $\sigma_o = bc_o / \pi R$

$$f(x_h, k) = 1 - x_h^3 - \frac{3k}{4} (1 - x_h^4)$$

The optimum distribution of  $\frac{CC_l}{R}$  can be determined from:

$$\frac{c C_l V_c}{R} = \Gamma \quad (10)$$

or substituting for  $\Gamma$  and  $V_c$  from equations (1) and (3) gives:

$$\frac{c C_l}{R} = \frac{8\pi F}{b} \omega_o' \sin \phi \quad (11)$$

For a uniformly tapered blade, the lift coefficient becomes:

$$C_{l_{avg}} = \frac{8 F w_o' \sin \phi}{\sigma_o (1 - k \lambda)} \quad (12)$$

### B. Application of Equations to Design of Rotor

It will be assumed that the blade airfoil section, planform, and tip speed are known from other considerations. Because of the profile drag losses, it is difficult to determine prior to the detailed calculations, the exact value of  $w_o'$  necessary to give the desired thrust coefficient. However, as a start, in equation 6(a) the factor  $F$  can be taken to be 1.0 and  $\epsilon = 0$  so that approximately:

$$\begin{aligned} C_T &\approx 2 w_o' \\ \text{or: } w_o' &\approx \sqrt{C_T/2} \end{aligned} \quad (13)$$

The procedure for applying the equations which have been developed thus far is perhaps better presented in steps.

1. Calculate  $w_o'$  from equation (13)
2. Calculate  $\phi$  from equation (1a)
3. Calculate  $F$  from equation (4)
4. Calculate  $CC_1$  from equation (11)
5. Knowing the chord distribution, the lift coefficients can be obtained from step 4 and then  $C_d$  from the airfoil section characteristics.
6. Calculate  $C_T$  and  $C_p$  from equation (6)
7. Steps 1 thru 6 are repeated until the desired  $C_T$  is obtained.
8. Calculate blade pitch angles from -

$$\beta = \phi + \frac{C_l}{a_0} \quad (14)$$

where:

$$a_0 = \frac{d C_l}{d \alpha}$$

### C. Selection of Optimum Rotor Parameters

The choice of the rotor solidity and thrust coefficient can be made on the basis of aerodynamic considerations. In so doing, the profile drag is the governing factor. In the absence of profile drag, the optimum rotor for supporting a given weight is obviously the largest one which can be tolerated. This follows, since from equation (6) for  $C_d = 0$  and  $F = 1.0$ :

$$C_P = 2 \left( \frac{C_T}{2} \right)^{3/2}$$

or

$$P = \frac{T^{3/2}}{\sqrt{2\rho\pi R^2}}$$

However, when the profile drag is included, there will be a point beyond which the increased loss in profile power will offset any decrease in induced power gained by increasing the radius.

To determine this optimum radius, the assumption is made that the angle  $\phi$  is small so that  $\cos \phi = 1$ . Then equation (5b) for the power can be written as:

$$P = 4\pi\rho R^2 V_T^3 \omega_o'^3 \int_{x_h}^1 x F dx + 4\pi\rho R^2 V_T^3 \omega_o'^2 \int_{x_h}^1 x^2 F E dx$$

It can be shown that, to the approximation that  $\phi$  is small:

$$F = \frac{\sigma_x C_d x}{8 \omega_o'^2}$$

where:  $\sigma_x = \frac{bc}{\pi R}$

thus: 
$$P = 4\pi\rho R^2 V_T^3 \omega_o'^3 \int_{x_h}^1 x F dx + \frac{\pi}{2} \rho R^2 V_T^3 \int_{x_h}^1 \sigma_x x^3 C_d dx$$

If equation (5a) is substituted for  $\omega_o'$  then:

$$P = \left[ \frac{T^{3/2}}{(4\pi\rho \int x F dx)^{1/2}} \right] \frac{1}{R} + \left[ \frac{\pi\rho V_T^3 \int x^3 \sigma_x C_d dx}{2} \right] R^2$$

This is of the form:

$$P = \frac{C_1}{R} + C_2 R^2$$

For a constant tip speed,  $T$ , and  $\sigma$ , the power will be a minimum when -

$$\frac{dP}{dR} = 0 = -\frac{C_1}{R^2} + 2C_2 R$$

or

$$R_{opt}^3 = C_1 / 2C_2$$

Notice that:

$$\frac{C_1}{R_{opt}} = 2 C_2 R_{opt}^2$$

That is, for minimum power, the induced power should be twice the profile power, a result which has been derived previously in reference (3). The expression for the optimum radius can be written as -

$$R_{opt}^3 = \frac{\left(\frac{T}{\rho V_T^2}\right)^{3/2}}{\pi \sigma_0 \left[ \int_0^1 x^3 (1-kx) C_d dx \right] \sqrt{4\pi \int_0^1 x F dx}} \quad (15)$$

Let:

$$\int_0^1 x^3 (1-kx) C_d dx = I_2$$

Equation (15) can be rewritten giving a relationship between the thrust coefficient and the solidity for minimum power.

$$\sigma_{opt} = \frac{C_{T_{opt}}^{3/2}}{2 I_2 \sqrt{\int_0^1 x F dx}} \quad (16)$$

It can be shown by expanding  $F$  in a series that:

$$\int_0^1 x F dx \cong \frac{1}{2} - \frac{19}{9\pi a}$$

where:  $a$

$$= \frac{b}{\sqrt{2C_T}}$$

If, in addition, it is assumed that the drag coefficient is a constant, then the following relationship can be obtained.

$$(1 - 0.8k) C_d \sigma_{opt} = \frac{2 C_T^{3/2}}{\sqrt{0.5 - \frac{0.672}{a}}} \quad (17)$$

If equation (9) for  $C_{l_{avg}}$  is substituted for  $\sigma_0$  in equation (17), then it will be found that -

$$\frac{(1 - 0.75k)}{(1 - 0.8k)} \frac{C_{l_{avg}}}{C_d} = \sqrt[3]{\frac{0.5 - \frac{0.672}{a}}{C_T}} \quad (18)$$

Equations (17) and (18) are plotted as a function of the thrust coefficient for different numbers of blades in Figure 2.

Before going to the optimum propeller, consider the implications of the foregoing development. The figure of merit of a rotor is defined as the ratio of the ideal induced power required by a rotor to hover to the actual power required.

$$M = \frac{P_i}{P_i + P_p}$$

where:  $P_i$  = induced power

$P_p$  = profile power

Most texts on helicopters, for example reference (4), state that  $M$ , for a good rotor, should be about 0.75. For the ideal rotor  $M = 1$ , while, according to reference (4),  $M = 0.5$  is poor for a rotor. But now consider  $M$  for the optimum rotor including profile drag. For this case it was just shown that the induced power should equal twice the profile power. Thus

$$M = \frac{2 P_p}{2 P_p + P_p} = \frac{2}{3}$$



The value of  $M = 0.667$  is rather unexpected and much lower than usually thought acceptable, and yet this is the value for a rotor requiring the least total power to produce a given thrust. Thus, the usual figure of merit for a rotor can be misleading and not a reliable basis for comparing different rotor designs.

A different standard for rotors in hovering is therefore proposed. Instead of using the ideal induced power as a basis for comparison it is proposed to use instead the power which would be required by the optimum rotor. For want of a better name, this new "figure of merit" will be called "design efficiency" and denoted by  $\eta_o$ .

$$\eta_o = \frac{P_{opt}}{P} \quad (19)$$

$$\text{Now } P \cong T w_o + \frac{\rho}{8} b c R V_T^3 C_d$$

$$P_{opt} = \frac{3}{2} T u_{opt}$$

so that:

$$\eta_o = \frac{w_{opt}}{\frac{2 w_o}{3} + \frac{\rho b c R V_T^3 C_d}{12 T}}$$

or

$$\eta_o = \frac{\frac{u_{opt}}{w_o}}{\frac{2}{3} + \frac{\rho b c R V_T^3 C_d}{12 T w_o}}$$

Now:

$$C_d \sigma_{opt} = 2\sqrt{2} \frac{w_{opt}}{T_{opt}}$$

and:  $w_0 = V_T \sqrt{\frac{C_T}{2}}$

so that:

$$\eta_0 = \frac{\gamma^{1/2}}{\frac{2}{3} + \frac{\gamma^{3/2}}{2}} \quad (20)$$

where:

$$\gamma = C_{T_{opt}} / C_T$$

Equation (20) is plotted as a function of  $\gamma$  in Figure 3. From this figure it can be seen that a rotor can be operating 20% off of the optimum  $C_T$  with only a 1% penalty in power.

#### D. The Optimum Propeller

A development will now be undertaken for the propeller similar to that which was just presented for the rotor. Consider the propeller blade element shown in Figure 4. In this development, the propeller will be assumed to be lightly loaded. Hence, the angle  $\alpha_i$ , the induced angle of attack, can be treated as a small angle. In the same manner as for the rotor, the thrust and torque force per blade can be written as:

$$dT = b \rho \Gamma (\alpha V_T - w_t) dr \quad (a) \quad (21)$$

$$dF = b \rho \Gamma (V + w_a) dr \quad (b)$$

where:  $V$  = inflow velocity

Again, for the optimum propeller, the Betz condition holds that  $w_0$ , the impact velocity, must be constant. Thus:

$$\tan \phi = \frac{V + w_o}{x V_T} = \frac{w_t}{w_a} = \frac{V + w_a}{x V_T - w_t} \quad (22)$$

Also:

$$b \Gamma = 4\pi r F w_t$$

The expressions for thrust and torque force therefore become:

(23)

$$dT = \frac{4\pi r F}{b} w_a (V + w_a) dr \quad (a)$$

$$dF_Q = dT \left( \frac{V + w_a}{x V_T} \right) \quad (b)$$

$$\text{or } dP = (V + w_o) dT \quad (c)$$

The ideal efficiency (neglecting profile drag) can be seen immediately to be,

$$\eta = \frac{TV}{P} = \frac{1}{1 + w_o/V}$$

Including the profile drag, the thrust and power coefficients become:

(24)

$$C_T = 4w_o' \int_{x_h}^1 F x \cos^2 \phi (\lambda + w_o' \cos^2 \phi) (1 - \epsilon \tan \phi) dx \quad (a)$$

$$C_P = 4w_o' \int_{x_h}^1 (\lambda + w_o') F x \cos^2 \phi (\lambda + w_o' \cos^2 \phi) (1 + \epsilon \tan \phi) dx \quad (b)$$

where:

$$\lambda = V/V_T$$

$$w_o' = w_o/V_T$$

$$\epsilon = C_d/C_l$$

As an approximation,  $w_o'$  and  $C_T$  are related by -

$$w_o' = \frac{1}{2} \left[ -\lambda + \sqrt{\lambda^2 + 2 C_T} \right] \quad (25)$$

### E. Selection of Optimum Propeller Parameters

The problem of choosing the solidity and radius for an optimum propeller is now considered. The power can be written as:

$$dP = (V + w_o') dT + \frac{b}{2} \rho V_e^2 C C_d \cos \phi x V_T R d\alpha$$

If the last term is called  $P_o$ , then

$$\begin{aligned} dP_o &= \frac{b}{2} \rho V_e^2 C C_d \cos \phi x V_T R d\alpha \\ &= \frac{b}{2} \rho V_e^2 C C_d \left( \frac{x V_T - w_t}{V_e} \right) x V_T R d\alpha \end{aligned}$$

If equation (19a) is substituted into the above then -

$$\begin{aligned} dP_o &= \frac{V_e}{2} \frac{C C_d dT}{\Gamma} \\ &= \frac{\sigma_x V_e V_T C_d dT}{8 x F w_t} \end{aligned}$$

$$\text{but } V_e = \frac{w}{\tan \alpha_i} = \frac{w_t}{\sin \phi \tan \alpha_i}$$

therefore:

$$dP_o = \frac{V_T \sigma_x C_d dT \cot \alpha_i}{8 x F \sin \phi}$$

The total power is thus:

$$dP = V dT + \frac{V_T \sin \alpha_i}{\cos \phi} + \frac{V_T \sigma_x C_d dT \cot \alpha_i}{8 x F \sin \phi}$$

If the elemental thrust is held constant, the elemental power will be a minimum when

$$\frac{dP}{d\alpha_i} = 0 = \frac{V_r \cos \alpha_{i_{opt}}}{\cos \phi} - \frac{\sigma_x C_d V_T}{8\pi F \sin \phi} \frac{1}{\sin^2 \alpha_{i_{opt}}}$$

$\alpha_i$  is small so that:

$$\alpha_{i_{opt}}^2 = \frac{\sigma_x C_d V_T \cos \phi}{8\pi F V_r \sin \phi}$$

If the value of  $\alpha_i$  is substituted into  $dP_o$  then

$$dP_o = \frac{V_r}{\cos \phi} \alpha_{i_{opt}} dT \quad (27)$$

but (27) is simply the induced power given by the second term in equation (26). Thus, for the optimum propeller with minimum power, the induced power should equal the profile power.

Thus:

$$P_{min} = (V + 2w_o)T \quad (28)$$

This result establishes an upper limit on the efficiency of a propeller with the profile drag included.

$$\eta_{max} = \frac{TV}{P_{min}} = \frac{1}{1 + 2w_o/V}$$

or, since  $\frac{w_o}{V}$  is given closely by

$$\frac{w_o}{V} = \frac{1}{2} \left[ -1 + \sqrt{1 + \frac{2C_r}{\lambda^2}} \right]$$

it follows that:

$$\eta_{max} = \frac{1}{\sqrt{1 + \frac{2 C_T}{\lambda^2}}} \quad (29)$$

A relationship between  $C_{T_{opt}}$ ,  $\sigma$  and  $\lambda$  can be obtained by writing the thrust coefficient approximately as:

$$C_T = \int_0^1 4x^2 F \lambda \alpha_i dx$$

and substituting from 26 for  $\alpha_i$ .

$$C_{T_{opt}} = \sqrt{2 \lambda \sigma_0} \int_0^1 \sqrt{C_d (1 - kx)} x^2 \sqrt{F \cos \phi} dx \quad (30)$$

An approximate relation between  $C_{T_{opt}}$ ,  $\sigma$  and  $\lambda$  can be obtained by letting  $k = 0$  (no taper) and assuming  $F = 1$  and  $C_d = \text{constant}$ .

$$\frac{C_{T_{opt}}}{\sqrt{C_d \sigma}} = \sqrt{2 \lambda} \int_0^1 \frac{x^{5/2}}{(x^2 + \lambda^2)^{1/2}} dx \quad (31)$$

The integral in equation (31) has been evaluated graphically as a function of  $\lambda$ . The result is presented in Figure 5. Also included in the figure are results obtained from reference (9) of experimental measurements with three-bladed variable pitch variable pitch propellers. For each collective pitch angle the value of the propeller advance ratio and thrust coefficient for maximum efficiency was chosen to give the point shown. The experimental trend is seen to be in substantial agreement with the theory.

F. Comparison of Optimum Rotor with the Optimum Propeller

The thrust coefficient of a VTOL rotor acting as a propeller can be expressed in terms of its coefficient as a rotor. If a sub "p" refers to propeller and a sub "r" to rotor, then

$$C_{T_P} = \frac{C_D}{C_L} \left( \frac{N_r}{N_P} \right)^2 C_{T_r} \quad (32)$$

where:  $C_D$  = aircraft drag coefficient  
 $C_L$  = aircraft lift coefficient  
 $N$  = rotational speed

The question is now posed as to whether equation (32) and Figures 2 and 5 can be satisfied simultaneously. Consider typical values of

$$\begin{aligned} C_{T_r} &= .016 \\ C_D/C_L &= 1/12 \\ \lambda &= .35 \end{aligned}$$

From Figure 2, for  $C_d = 0.01$ ,  $\sigma_{opt} = 0.58$

From Figure 5,  $C_T / \sqrt{C_d \sigma} = .0198$

therefore:

$$N_P / N_r = 0.284$$

In terms of the usual rotor tip speeds, this would give a very low  $N_P$  and, hence, for this  $\lambda$  a very low aircraft speed.

Increasing  $C_T$  does not change this result appreciably. Now choose  $\lambda = 1.0$ . Then  $C_{T_P} = .43 \sqrt{C_d \sigma}$  or  $C_{T_P} = .0327$

therefore:  $N_P / N_r = 0.221$

Again even for this relatively high  $\lambda$ , for the usual rotor tip speeds, this results in low aircraft speeds. Actually, the value of  $C_{Tp}/\sqrt{C_d \sigma}$  for  $\lambda$  larger than 1 should not change much beyond the value of 0.4. Thus  $\frac{N_p}{N} = 0.22$  and  $\lambda \cong 5$  would be needed in order for both the rotor and propeller to be compatible with optimum requirements.

From these examples, it does not appear feasible to attempt a design which would have an optimum solidity as both a rotor and a propeller. Therefore attention will now be given to the problem of analyzing a given rotor or propeller.

#### G. Analysis of Given Rotor or Propeller

Reference is again made to Figure 4. Now, instead of finding the  $\beta$  distribution to give the optimum induced velocity distribution, the  $\beta$  will be given. The problem then is to find the induced velocity and hence the lift and drag coefficients for given  $V$  and  $V_T$  values. To do this, the bound circulation,  $\Gamma$ , is written first as:

$$\Gamma = \frac{1}{2} C C_l V_e$$

but  $\Gamma$  is also given approximately by:

$$\Gamma = \frac{4\pi r F \omega_t}{b}$$

Equating the two expressions for  $\Gamma$  gives

$$C_l = \frac{8\pi F \omega_t}{\sigma_x V_e} \quad (33)$$

but  $C_l$  is also given by:

$$C_l = a_o (\beta - \phi) \quad (34)$$



so that

$$a_o(\beta - \phi) = \frac{8\lambda F w_t}{\sigma_x V_e}$$

From the geometry of Figure 4, it can be seen that -

$$w_t = V_e \tan \alpha_i \sin \phi \quad (35)$$

Thus:

$$a_o(\beta - \theta - \alpha_i) = \frac{8\lambda F}{\sigma_x} \tan \alpha_i \sin \phi$$

now:

$$\phi = \tan^{-1} \frac{\lambda}{x} + \alpha_i$$

Thus the induced angle of attack is given implicitly by:

$$a_o(\beta - \theta - \alpha_i) = \frac{8\lambda F}{\sigma_x} \tan \alpha_i \sin \left[ \tan^{-1} \frac{\lambda}{x} + \alpha_i \right] \quad (36)$$

This equation can be solved explicitly to the approximation that  $\alpha_i$  is small:

$$\sigma_x a_o(\beta - \theta - \alpha_i) = 8\lambda F \alpha_i (\sin \theta + \alpha_i \cos \theta)$$

Therefore:

$$\alpha_i = \frac{1}{2} \left[ -B + \sqrt{B^2 + 4C} \right] \quad (37)$$

$$\text{where: } B = \tan \theta + \frac{\sigma_x a_o}{8\lambda F \cos \theta}$$

$$C = \frac{\sigma_x a_o (\beta - \theta)}{8 \chi F \cos \theta}$$

For a rotor in hovering  $\lambda = 0$  so that  $\theta = 0$ .

For this case, the induced angle of attack becomes:

$$\alpha_i = \frac{\sigma_x a_o}{16 \chi F} \left[ \sqrt{1 + 4 \left( \frac{8 \chi F}{\sigma_x a_o} \right) \beta} - 1 \right] \quad (38)$$

The tip loss factor  $F$  is given by (4). The angle  $\phi_T$  in equation (4) can be taken to be  $\beta_T$ , the blade pitch angle at the tip.

Thus knowing  $\beta$ ,  $\sigma_x$ ,  $\lambda$  and the airfoil section characteristics, the radial variation of  $\alpha_i$  can be calculated. The section lift coefficients are then obtained from (34).

The thrust and power coefficients can be calculated by:

$$C_T = \frac{T}{\rho V_T^2 \pi R^2} = \frac{1}{2} \int_0^1 \sigma_x \left( \frac{V_e}{V_T} \right)^2 C_L \cos \phi (1 - \epsilon \tan \phi) d\chi \quad (a)$$

$$C_P = \frac{P}{\rho V_T^3 \pi R^2} = \frac{1}{2} \int_0^1 \chi \sigma_x \left( \frac{V_e}{V_T} \right)^2 C_L \sin \phi (1 + \epsilon \cot \phi) d\chi \quad (b)$$

The velocity  $(V_e/V_T)$ , to the approximation of  $\alpha_i$  being small, is given closely by:  $\left( \frac{V_e}{V_T} \right)^2 = \lambda^2 + \chi^2$

H. Results of Digital Computer Program

An extensive program has been performed on an IBM Model 650 magnetic drum digital computer. The program considered only rotors or propellers having constant pitch; that is, with blade pitch angles given by:

$$\beta = \tan^{-1} \frac{P/D}{\pi \chi} + \Delta\beta \quad (40)$$

where:  $p$  = propeller pitch

$\Delta\beta$  = propeller collective pitch angle.

This particular pitch distribution was chosen when it was found to agree closely with the  $\beta$  distributions calculated for the optimum rotors or propellers for  $\Delta\beta = 0$ .

The drag coefficient variation with Mach No. was taken proportional to the fourth power of the difference between the critical Mach No. and the local operating Mach No. This is in accordance with the recommendation of references (5) and (6). Specifically, the drag coefficient was expressed as:

$$\begin{aligned} C_d &= C_{d_0} + C_2 C_l^2 & M \leq M_{cr} \\ &= C_{d_0} + C_2 C_l^2 + K (M - M_{cr})^4 & M > M_{cr} \end{aligned}$$

The critical Mach No. is given approximately by:

$$M_{cr} = M_{cr_0} - m_1 C_l$$

where:  $C_2$ ,  $K$ , and  $m_1$  are constants of proportionality

$C_l$  = section lift coefficient

$$C_{d_0} = C_d \text{ for } C_l = 0$$

$$M_{cr_0} = \text{critical Mach No. for } C_l = 0$$

For the 12% thick series 16 airfoils which were used in this study, the various constants were determined from reference (7) as:

$$C_2 = 0.006$$

$$K = 200$$

$$m_1 = 0.162$$

$$M_{cr_0} = 0.757$$

$$C_{d_0} = 0.006$$

The slope of the section lift coefficient curve was corrected for compressibility effects by fitting the empirical results of reference (8) with the following expression:

$$a_0 = a_{0inc} (1 + a_4 M^4 + a_{10} M^{10})$$

The constant  $a_4$  and  $a_{10}$  were found to be:

$$a_4 = 1.438$$

$$a_{10} = -4.29$$

$a_{0inc}$  is the slope of the lift curve for incompressible flow and for a 12% thick series 16 airfoil was taken as  $a_{0inc} = 4.8$ .

The effect of Reynold's No. was not considered in these calculations. The Reynold's No. for the test data of reference (7) was between  $0.85 \times 10^6$  and  $2 \times 10^6$ . As long as the Reynold's number of an average propeller station, say the 0.7 radius, is of this order the results given here should be valid.

The basic results which were obtained are presented in Figures 6 through 16. Figure 6 presents the calculated thrust and power coefficients of families of rotors having constant pitch with  $\Delta\beta = 0$ . These curves represent about the best performance that could be obtained with a hovering rotor since the aerodynamic loading is close to ideal and their airfoil sections are very clean. These results are all for a constant tip Mach No. of 0.75.

The effect of tip Mach No. on a hovering rotor as predicted by the present methods is shown in Figure 7. For a given thrust coefficient, the power coefficient is seen to be nearly the same for  $M_T = .8$  as for  $M_T = .6$ , since for a given pitch-diameter ratio both the thrust and power coefficients are higher for  $M_T = 0.8$ . For a tip Mach No. of 0.9 the performance of the rotor is seen to be seriously affected. The thrust coefficient, for a given P/D, is lower than that of  $M_T = .8$  while the power coefficient is appreciably higher.

Figures 8, 9 and 10 present the calculated thrust and power coefficient as a function of the collective pitch angle for propellers whose P/D values were chosen from Figure 6 to have average  $C_1$  values in hovering of 0.5. As noted on the figures, the performance of the propeller was calculated for three different values of the forward speed-tip speed ratio,  $\lambda$ .

The calculated performance of constant pitch propellers with  $\Delta\beta = 0$  for different  $\lambda$  values is presented in Figures 11, 12 and 13. These curves are all calculated at a constant forward

CONFIDENTIAL

Page 28  
Report R-77

Mach No. of 0.4.

Figures 14, 15 and 16 present the calculated performance of the propellers of the previous three figures when performing as rotors. The P/D values were chosen such that, as propellers with  $\Delta\beta = 0$ , the thrust coefficient would be 0.005.

CONFIDENTIAL

3

V. CONCLUSIONS

Although it appears difficult to state any definite rules for the selection of a VTOL propeller, there are some general observations and conclusions that can be made from the results of this study. From the analyses of the optimum rotor and the optimum propeller, it appears impossible to attain both of these optimums in a single design. However, certain design practices can be followed which should assure a good aerodynamic compromise between the states of operation.

These practices are evident from Figures 17 and 18. These figures have been constructed from the results given in Figures 6 through 16. Figure 17 presents the power required by the optimum rotor acting as a propeller to deliver a given thrust coefficient as compared with the power required by the optimum propeller to deliver the same thrust coefficient. Figure 18 presents the power required by the optimum propeller to hover at a given thrust coefficient compared with the power required by the optimum rotor.

Regardless of whether the VTOL propeller is designed as an optimum propeller or as an optimum rotor or as a compromise, one important fact is obvious from both Figures 17 and 18. The ratio,  $\lambda$ , of the propeller forward speed to the tip speed should be relatively high. The gain in power from increasing  $\lambda$  is two-fold. Not only does the ratio of power coefficients decrease with increasing  $\lambda$  at a constant  $C_t$  value but, in addition, for a given thrust and forward speed, the  $C_t$  value increases with increasing  $\lambda$  which further reduces the ratio of power

coefficients. There is a limit, of course, to the value of  $\lambda$  above which the power required to produce a given thrust at a certain forward speed will increase. This optimum  $\lambda$  can be estimated from Figure 5.

Another conclusion of some significance is to be drawn from these figures. This can best be shown by considering a typical example. Assume a tilt-wing VTOL transport with the following characteristics:

gross weight	100,000#
forward velocity	400 fps
number of propellers	4
average $C_1$ in hovering	0.5
drag in forward flight	10,000#

The power required to hover using an optimum rotor and an optimum propeller is shown as a function of the propeller advance ratio for different values of solidity in Figure 19. The power required for forward flight for the optimum propeller and optimum rotor is given in Figure 20 as a function of  $\lambda$ . Now it is felt that because of weight and other considerations, the blade solidity of a VTOL aircraft will be high in comparison with the usual helicopter rotor. From Figure 19, it can be seen that over the range of values considered, the power required to hover by the propeller for solidities of 0.3 and 0.5 is at the most, only 4% higher than the power required by the optimum rotor. However, from Figure 20, the power required by the optimum rotor in forward flight is at least 10% higher than that required by the optimum propeller at the higher  $\lambda$  values and at the lower values of  $\lambda$  is more than 50% higher than for the propeller.



CONFIDENTIAL

Page 31  
Report R-77

Thus, it would appear advisable in designing the VTOL propeller, that is in selecting the blade twist and planform, to favor the operation of the propeller in the airplane state.

VI. REFERENCES

1. S. Goldstein, "On the Vortex Theory of Propellers", Proc. of Royal Society A123, 440, (1929)
2. W. F. Durand, "Aerodynamic Theory", Vol. IV Division L (1943)
3. W. Z. Stepniewski, "Introduction to Helicopter Aerodynamics", Vol. I, Chapter VI, Rotorcraft Publishing Committee (1950)
4. A Gessow, and Myers, G. C., "Aerodynamics of the Helicopter", MacMillan Company (1952)
5. W. F. Hilton, "High Speed Aerodynamics", Longmans, Green and Company (1951)
6. Hoerner, S. F., "Aerodynamic Drag", published by author (1951)
7. Lindsay et. al, "Aerodynamic Characteristics of 24 NACA 16-Series Airfoils at Mach Numbers between 0.3 and 0.8", NACA TN-1546 (1948)
8. Eggers, A. J., "Aerodynamic Characteristics at Sub-Critical and Super Critical Mach Numbers of Two Airfoil Sections Having Sharp Leading Edges and Extreme Rearward Position of Maximum Thickness", NACA RM No. A7C10 (1947)
9. Biermann, D. and Hartman, E. P., "Tests of Two Full Scale

CONFIDENTIAL

Page 33  
Report R-77

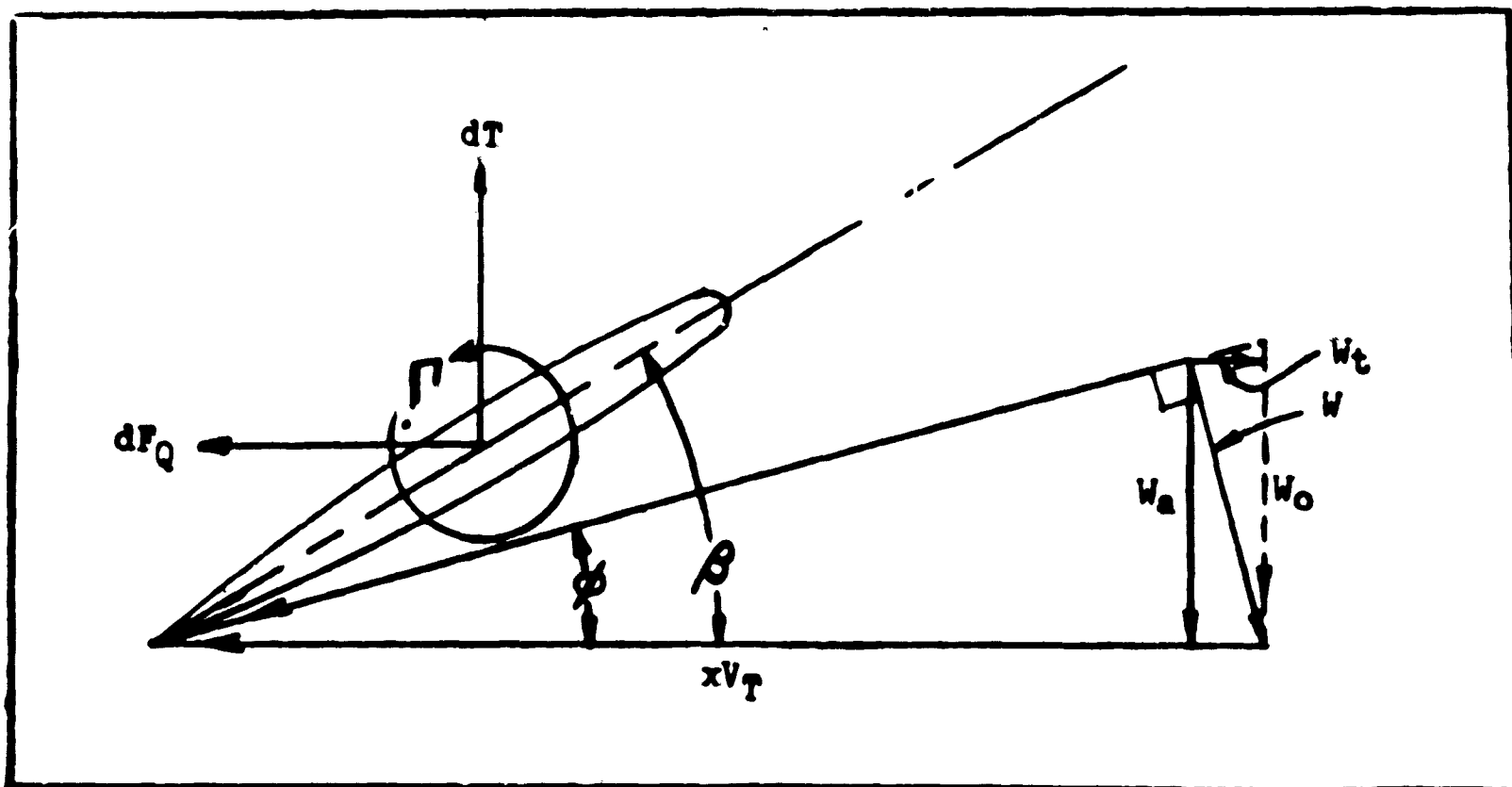
Propellers with Different Pitch Distributions, at Blade  
Angles up to  $60^\circ$ , NACA TR-658

CONFIDENTIAL

CONFIDENTIAL

Page 34  
Report R-77

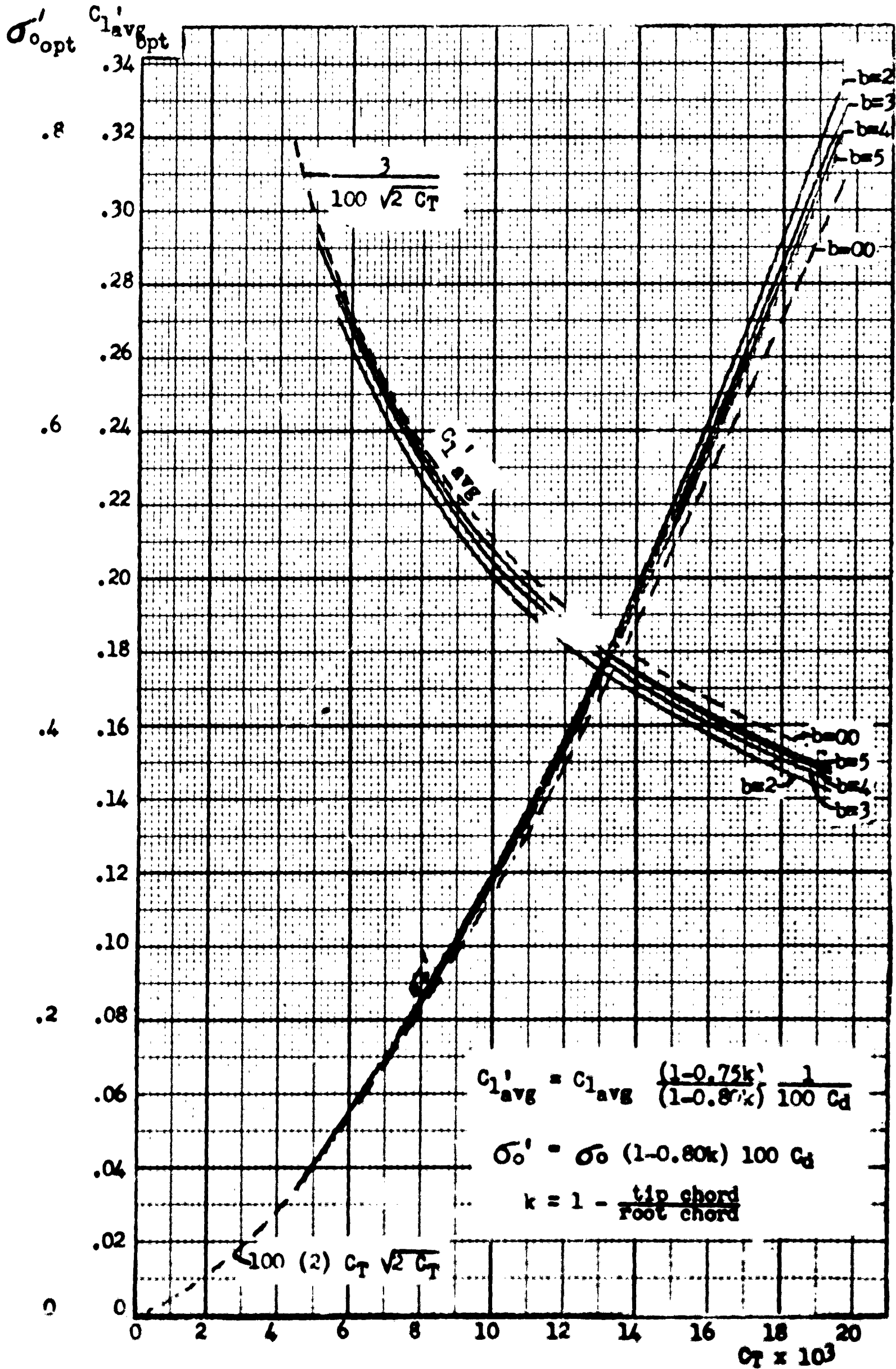
FIGURE 1  
ROTOR BLADE ELEMENT IN HOVERING



CONFIDENTIAL

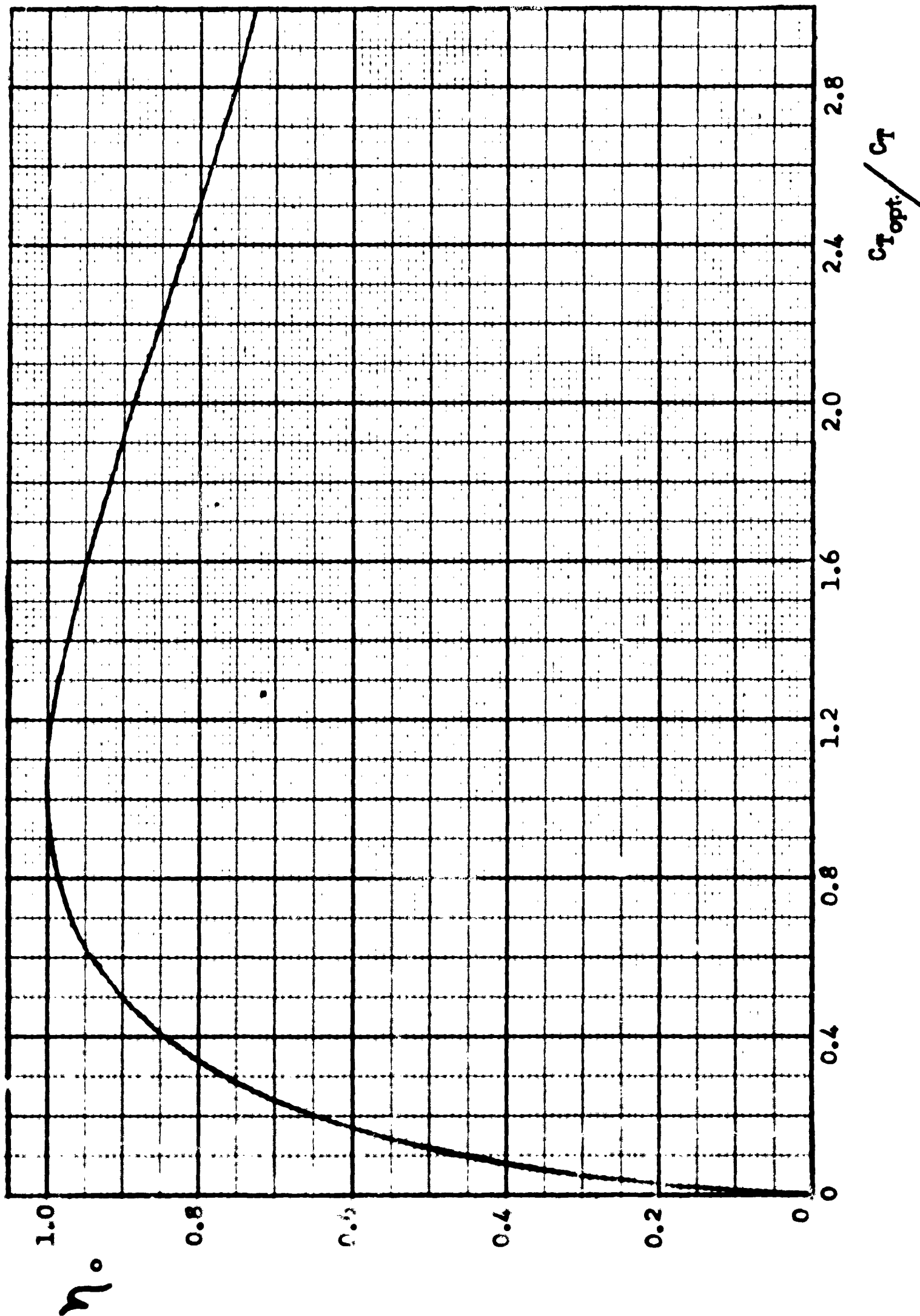
FIGURE 2

RELATIONSHIP BETWEEN OPTIMUM SOLIDITY, THRUST COEFFICIENT  
AND AVERAGE LIFT COEFFICIENT FOR A ROTOR



Optimum  $\sigma_0$  &  $Cl_{avg}$  vs  $CT$  for Linearly Tapered Optimum Rotor in Hovering  
CONFIDENTIAL

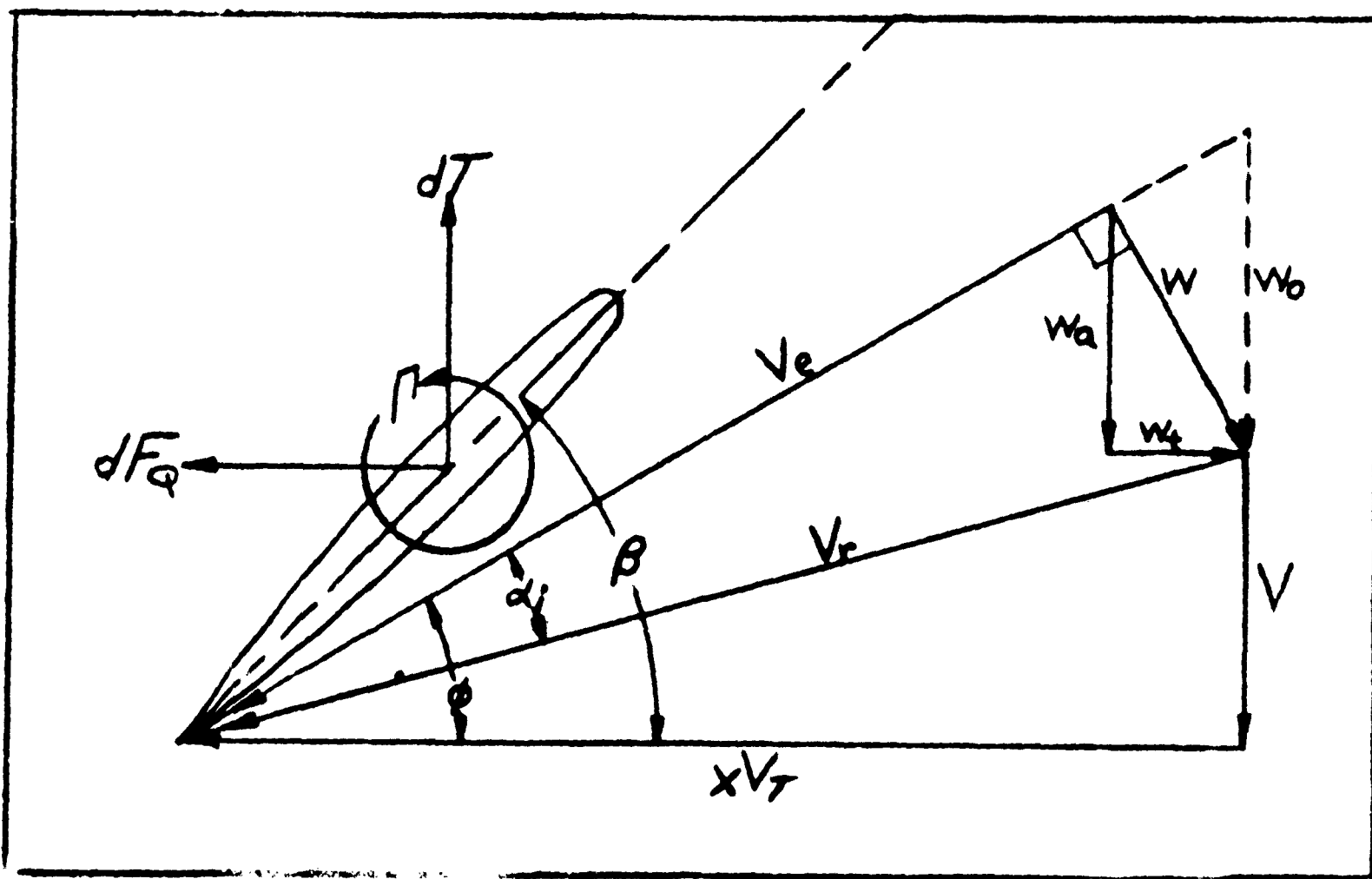
FIGURE 3  
DESIGN EFFICIENCY



CONFIDENTIAL

Page 37  
Report R-77

FIGURE 4  
PROPELLER BLADE ELEMENT



CONFIDENTIAL

FIGURE 5  
RELATIONSHIP BETWEEN OPTIMUM SOLIDITY, THRUST  
COEFFICIENT AND  $\lambda$  FOR A PROPELLER

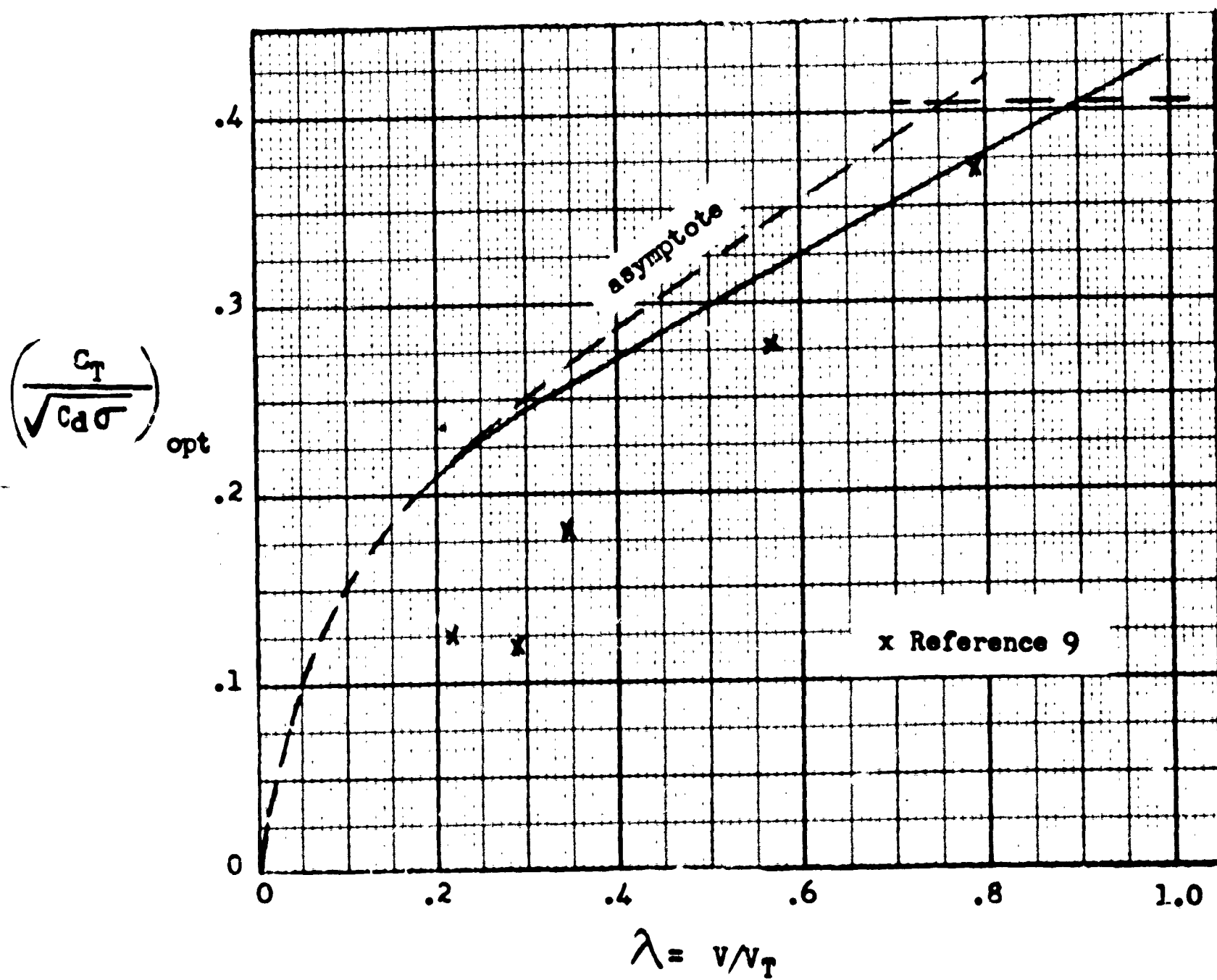




FIGURE 6  
CALCULATED PERFORMANCE OF CONSTANT - PITCH ROTORS

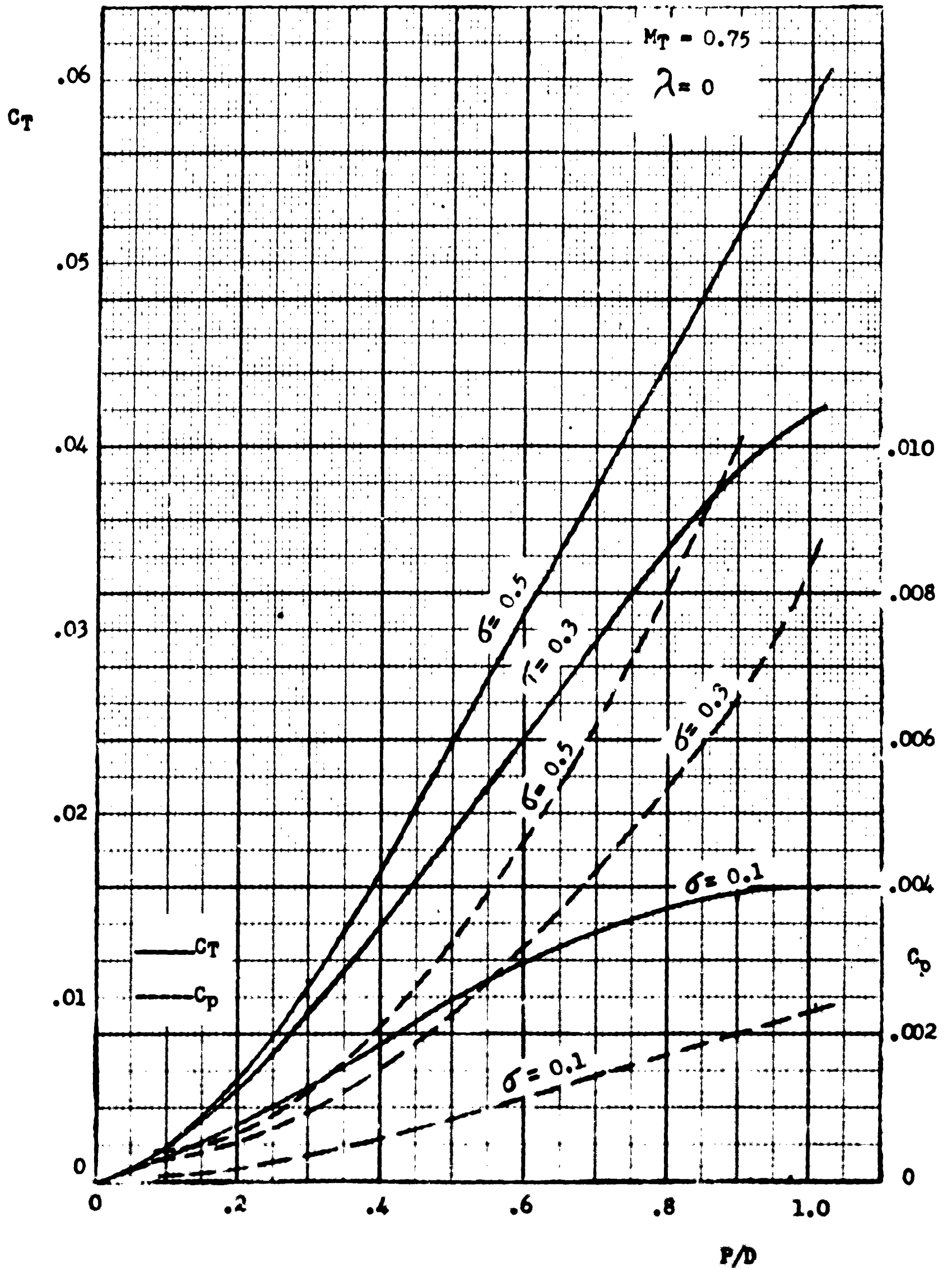


FIGURE 7  
EFFECT OF MACH NUMBER ON THE PERFORMANCE OF CONSTANT PITCH ROTORS

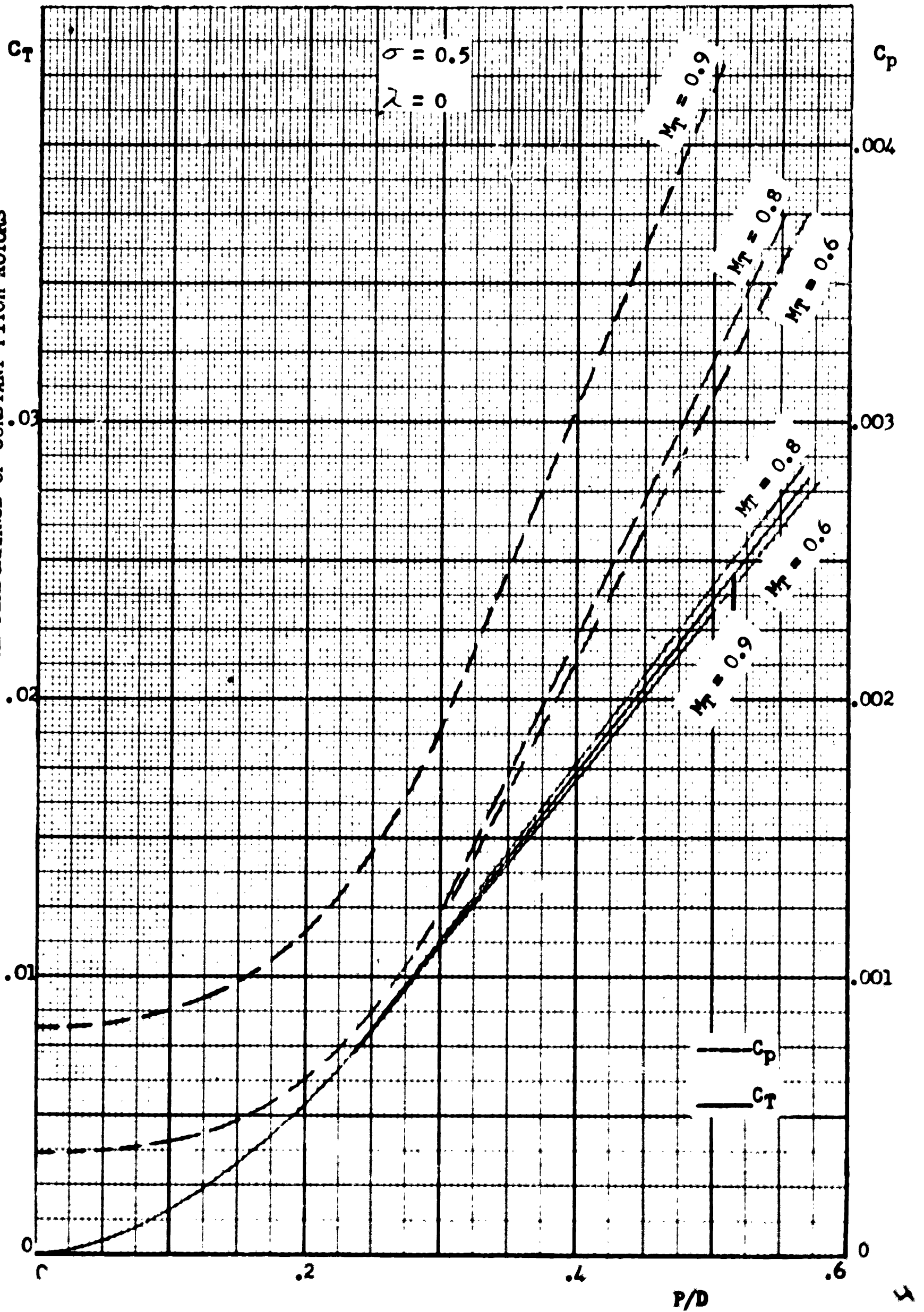


FIGURE 8  
CALCULATED PERFORMANCE OF CONSTANT - PITCH ROTORS  
WITH  $C_{l_{avg}} = 0.5$  ACTING AS PROPELLERS

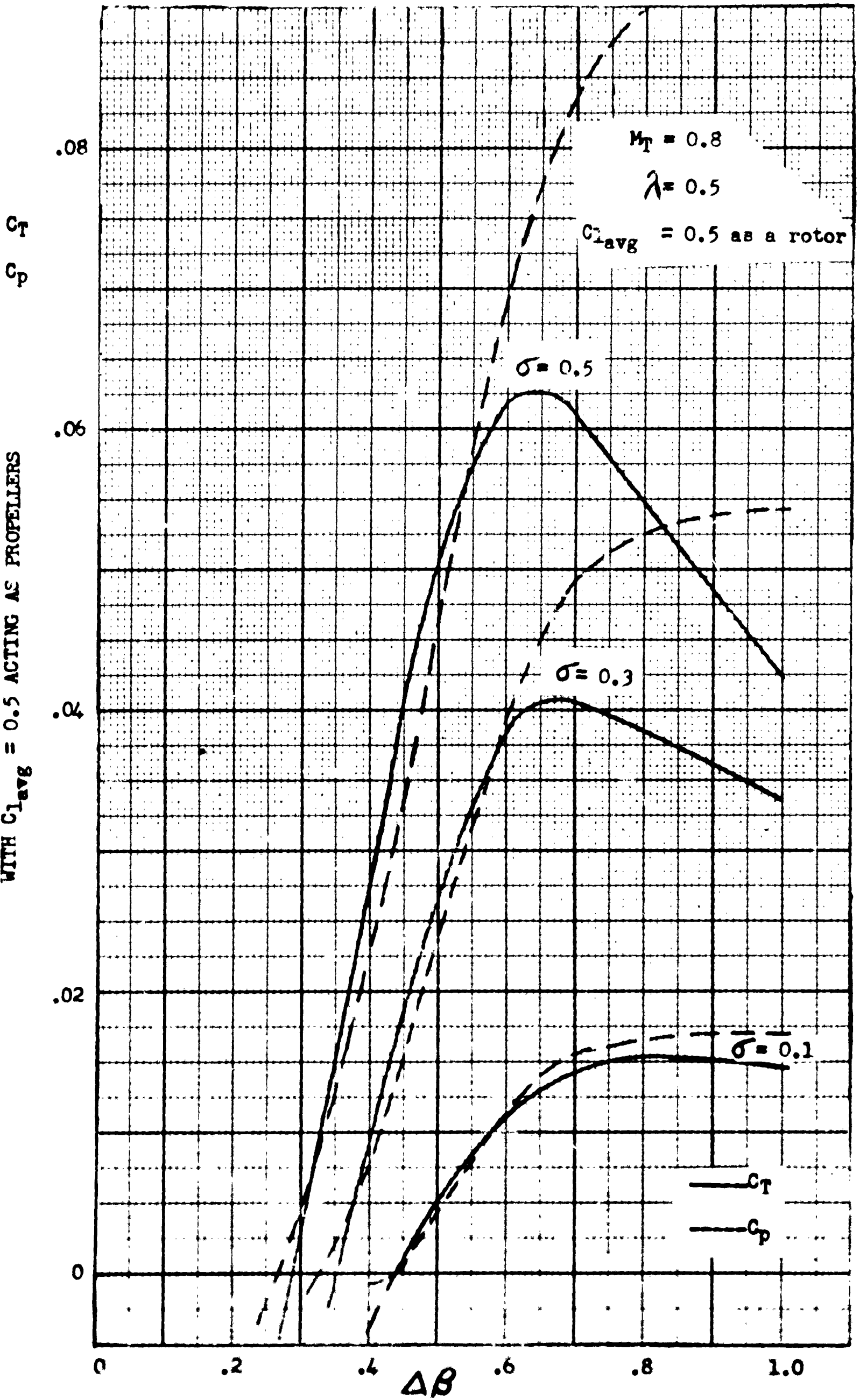


FIGURE 9  
CALCULATED PERFORMANCE OF CONSTANT - PITCH ROTORS  
WITH  $C_{l_{avg}} = 0.5$  ACTING AS PROPELLERS

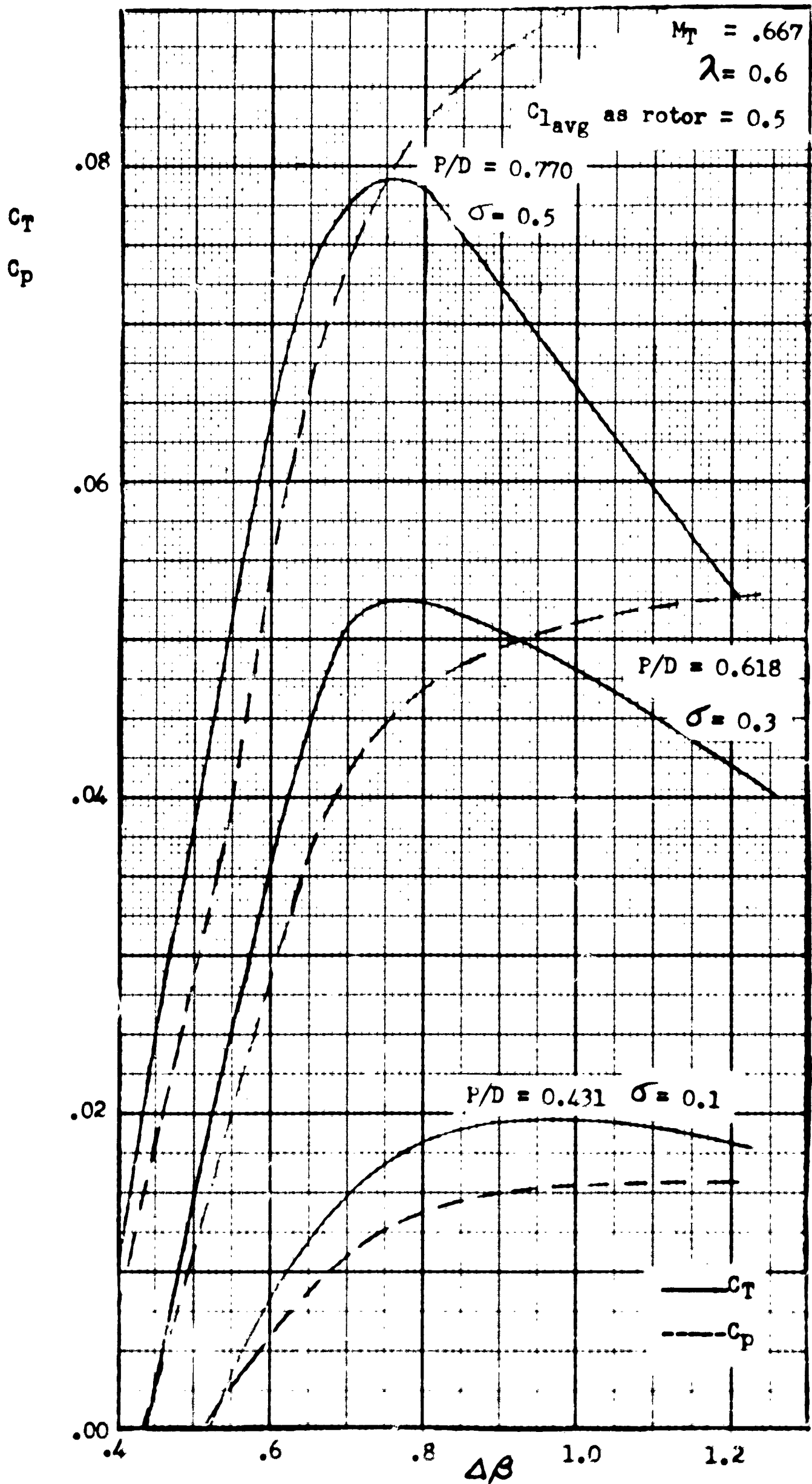


FIGURE 10  
CALCULATED PERFORMANCE OF CONSTANT - PITCH ROTORS  
WITH  $C_{l_{avg}} = 0.5$  ACTING AS PROPELLERS

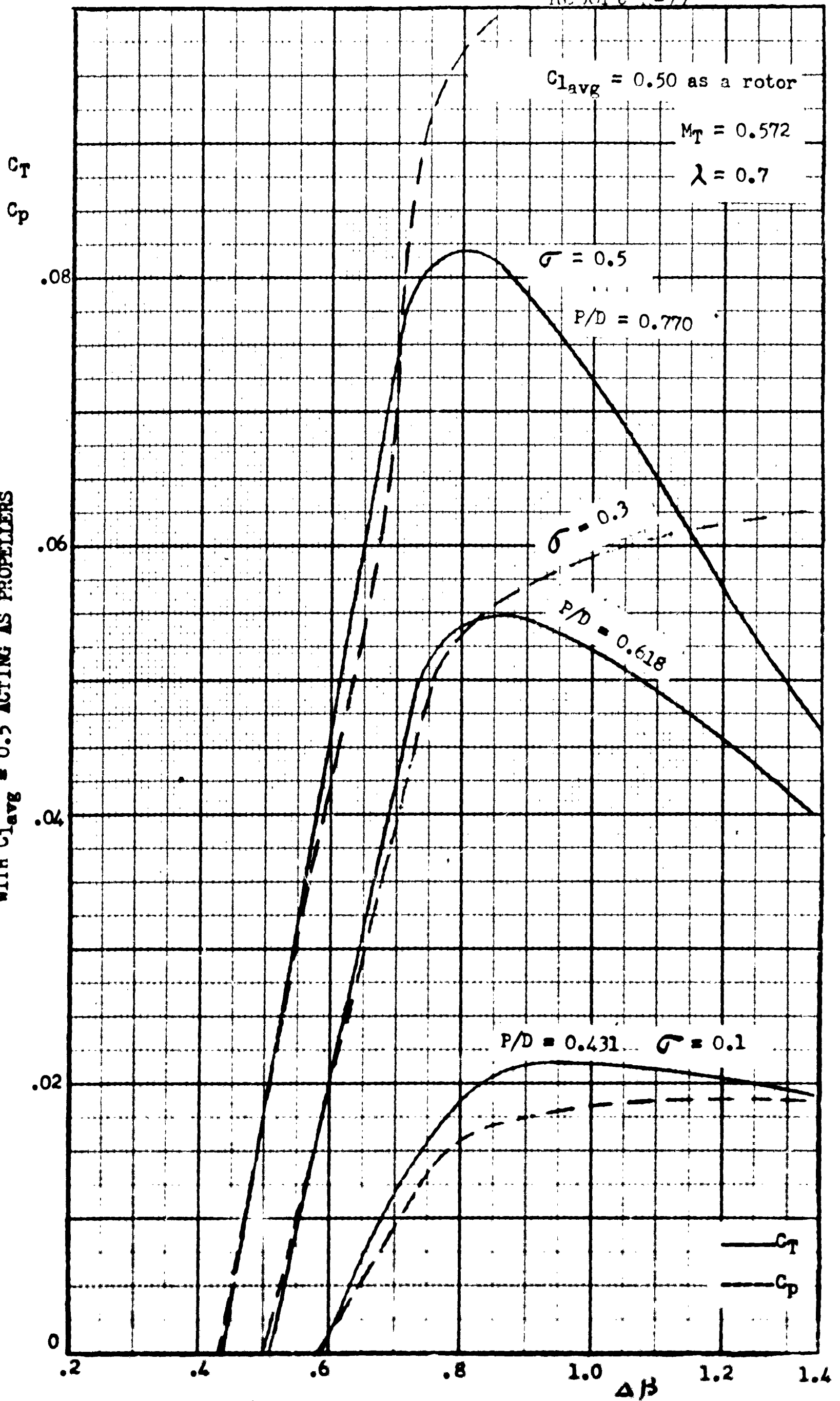


FIGURE 11  
CALCULATED PERFORMANCE OF CONSTANT - PITCH PROPELLERS

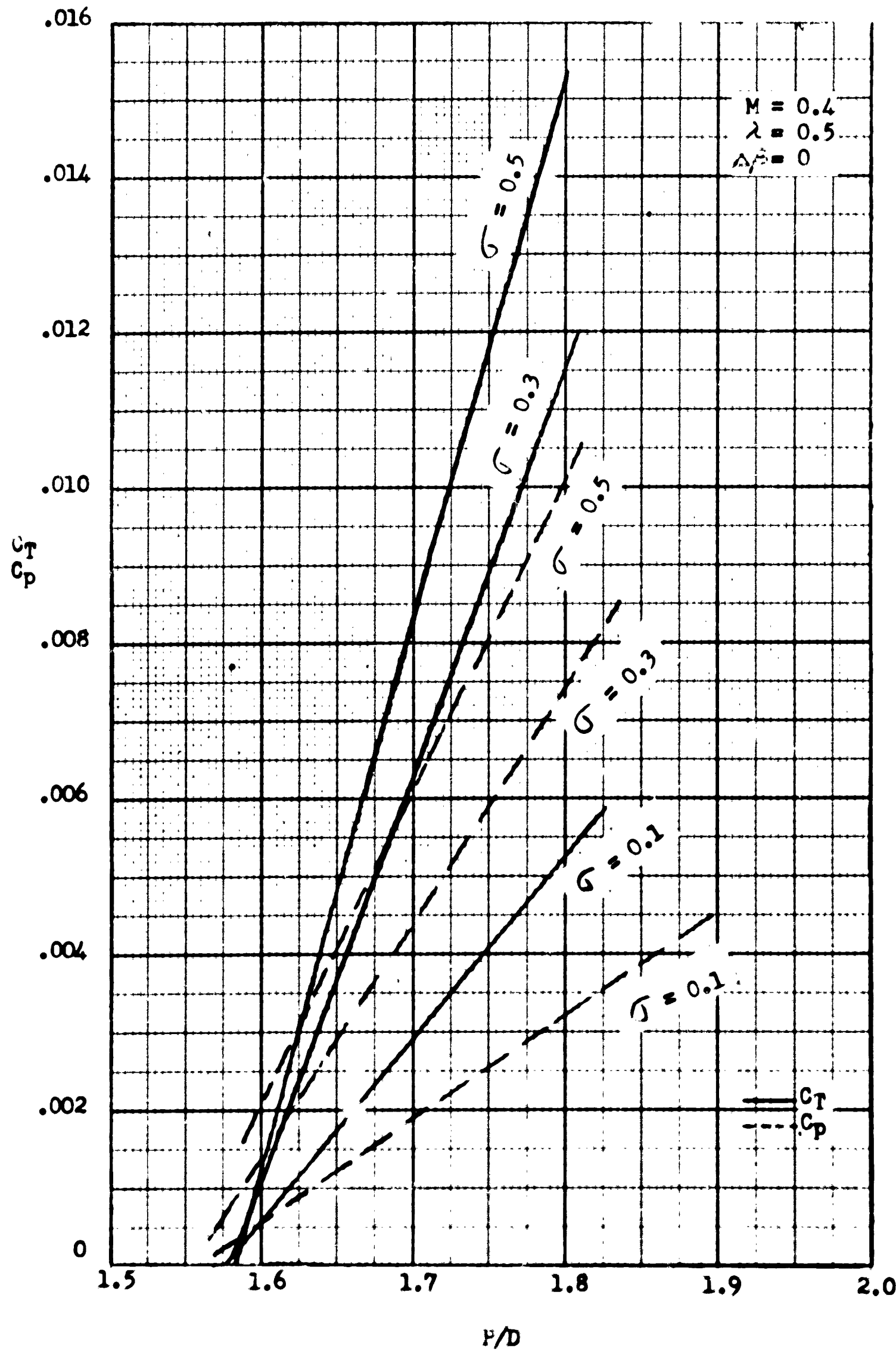


FIGURE 12

## CALCULATED PERFORMANCE OF CONSTANT - PITCH PROPELLERS

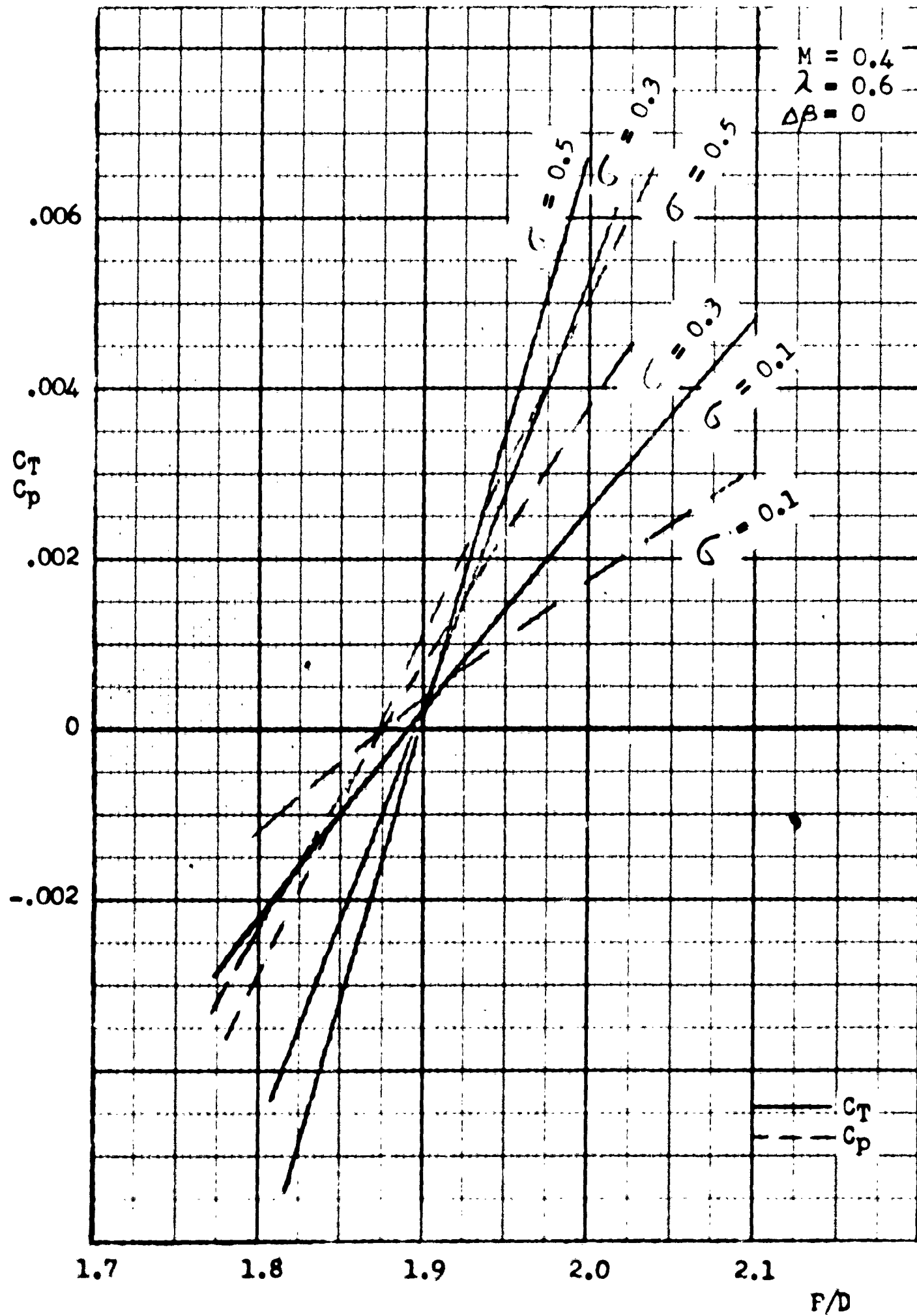




FIGURE 13

CALCULATED PERFORMANCE OF CONSTANT - PITCH PROPELLERS

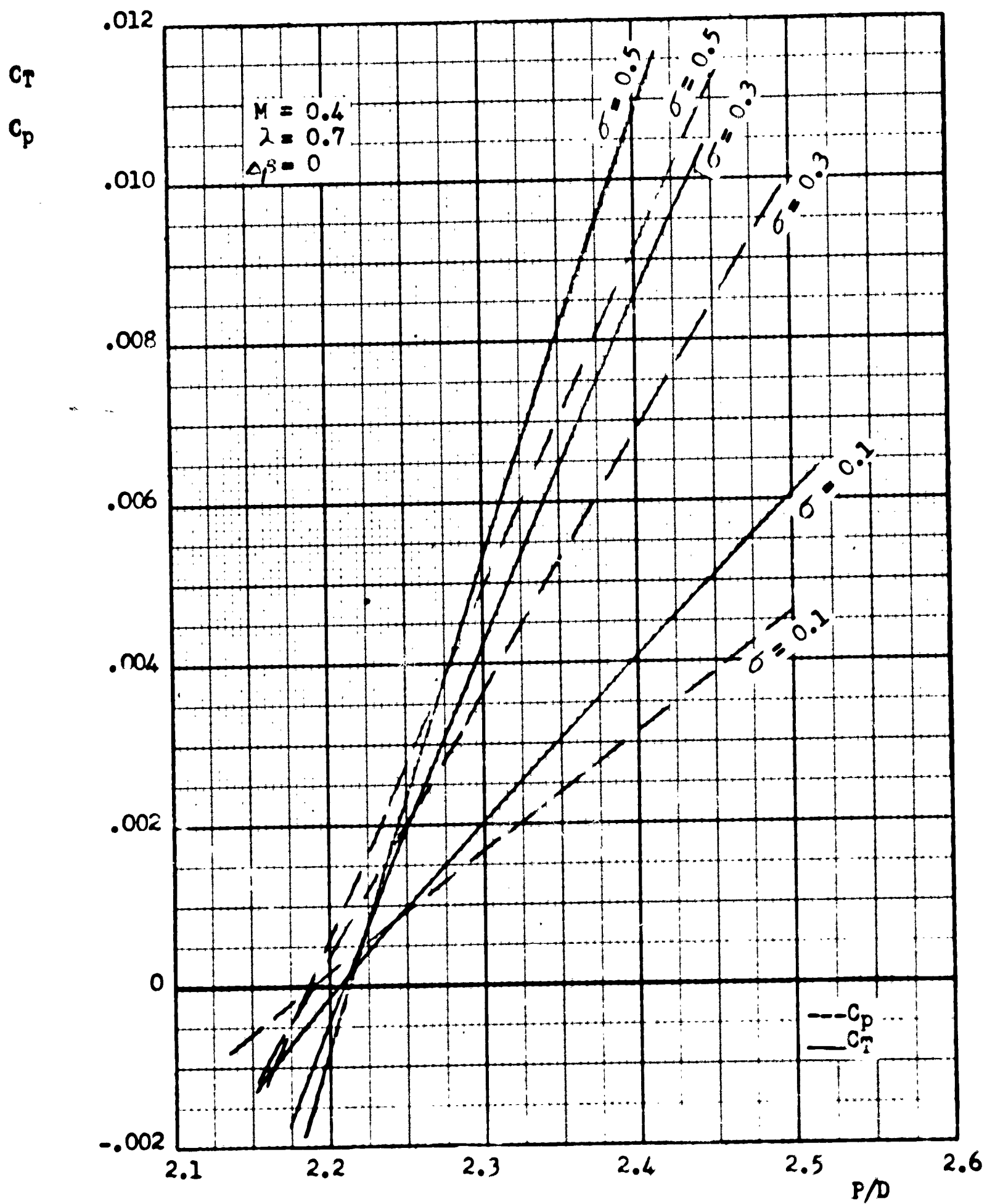




FIGURE 14  
CALCULATED PERFORMANCE OF CONSTANT - PITCH PROPELLERS  
WITH  $C_T = .005$  ACTING AS ROTORS ( $\lambda = 0.5$ )

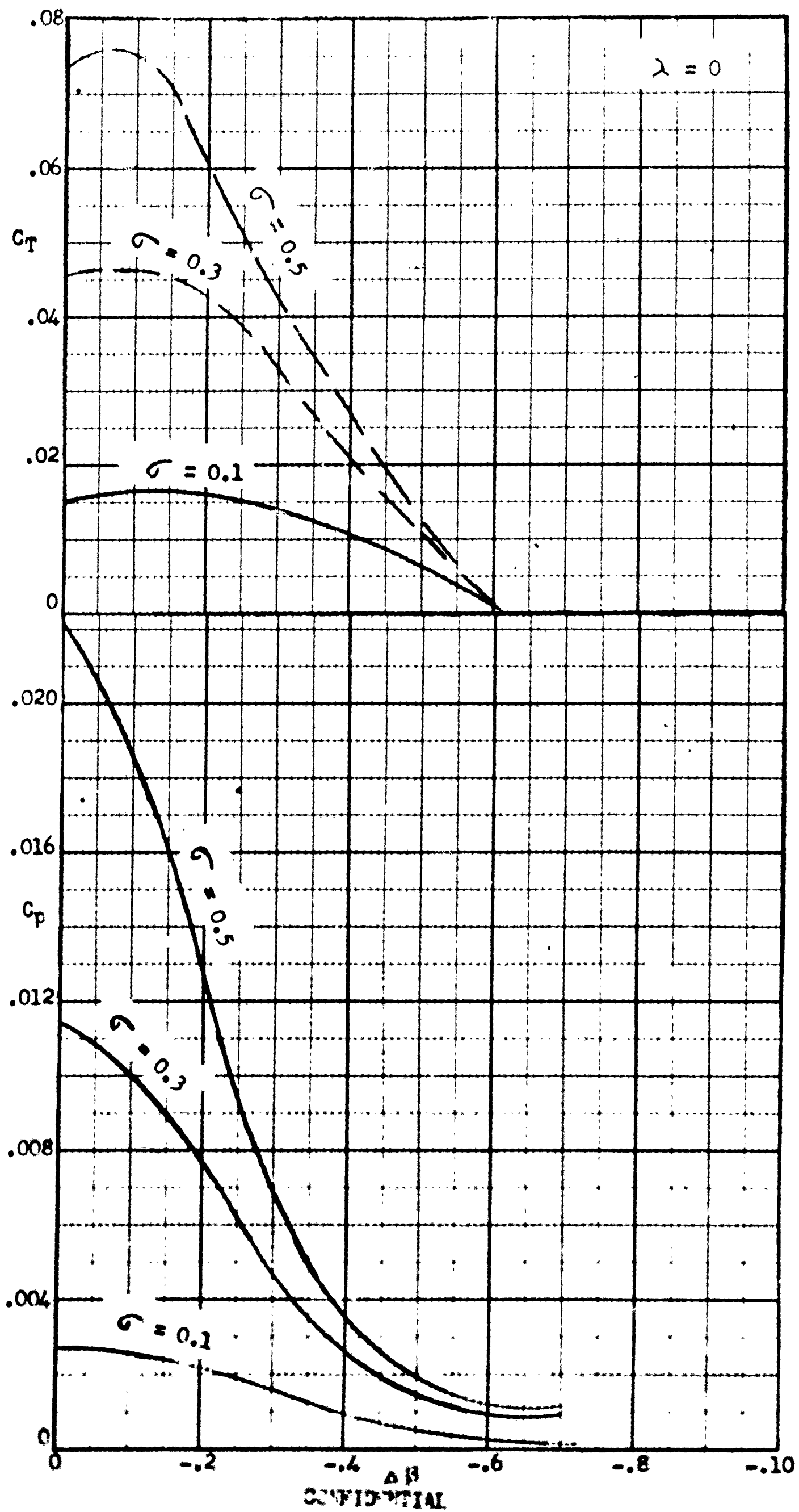


FIGURE 15  
CALCULATED PERFORMANCE OF CONSTANT - PITCH PROPELLERS  
WITH  $C_T = .005$  ACTING AS ROTORS ( $\lambda = 0.6$ )

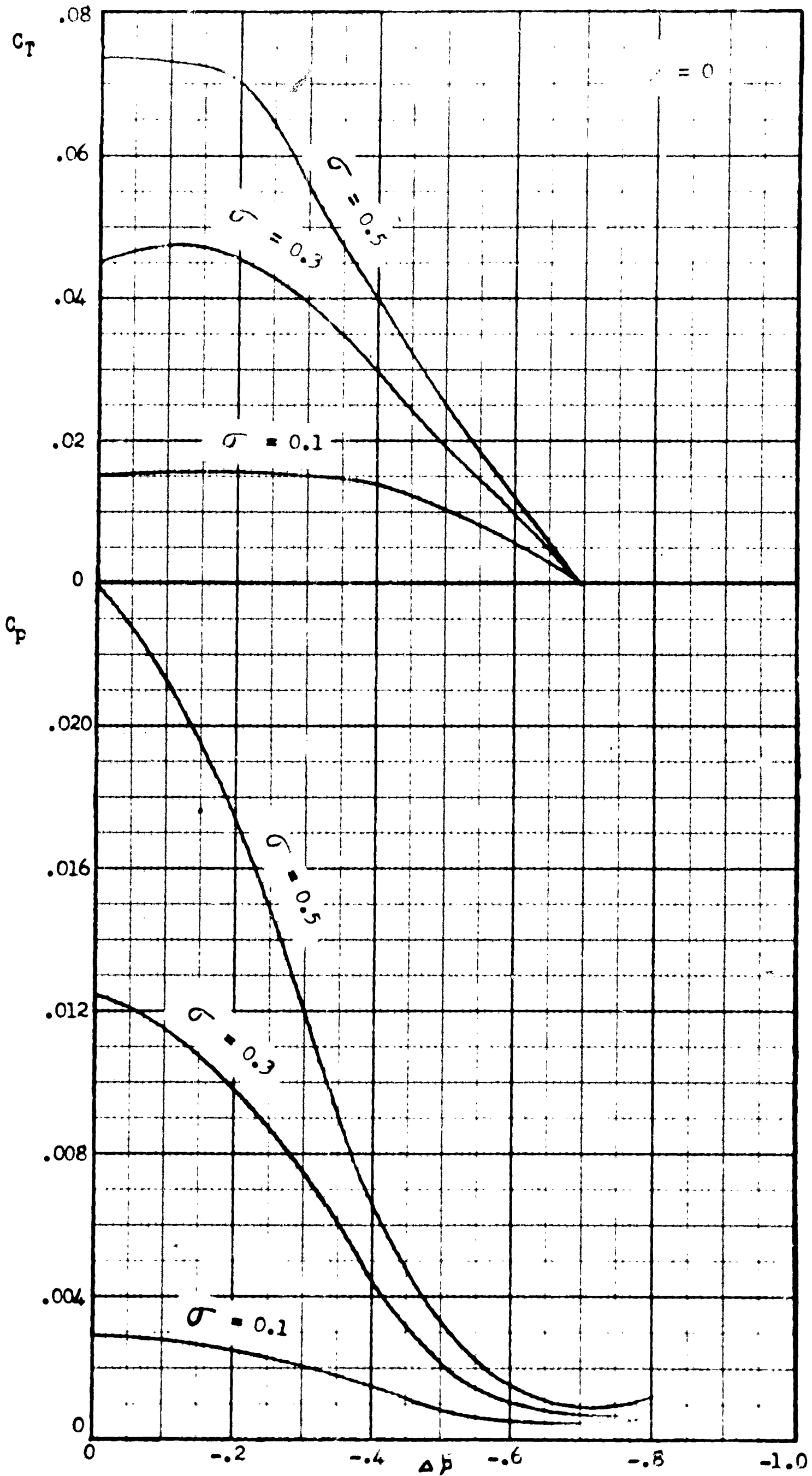


FIGURE 16  
CALCULATED PERFORMANCE OF CONSTANT - PITCH PROPELLERS  
WITH  $C_T = .005$  ACTING AS ROTORS ( $\lambda = 0.7$ )

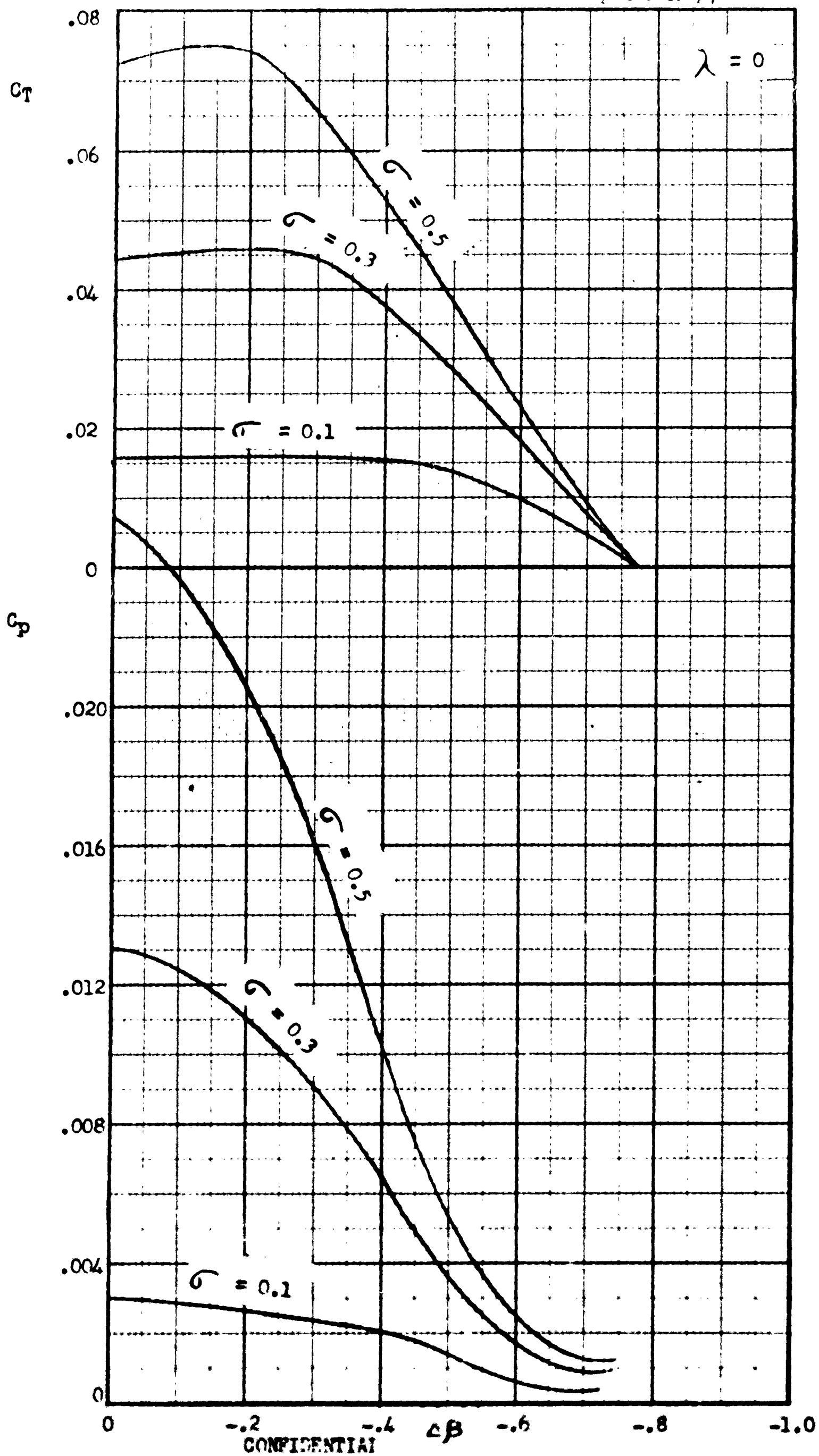


FIGURE 17

COMPARISON OF POWER REQUIRED BY AN OPTIMUM ROTOR AND AN  
OPTIMUM PROPELLER WITH BOTH PERFORMING AS A PROPELLER

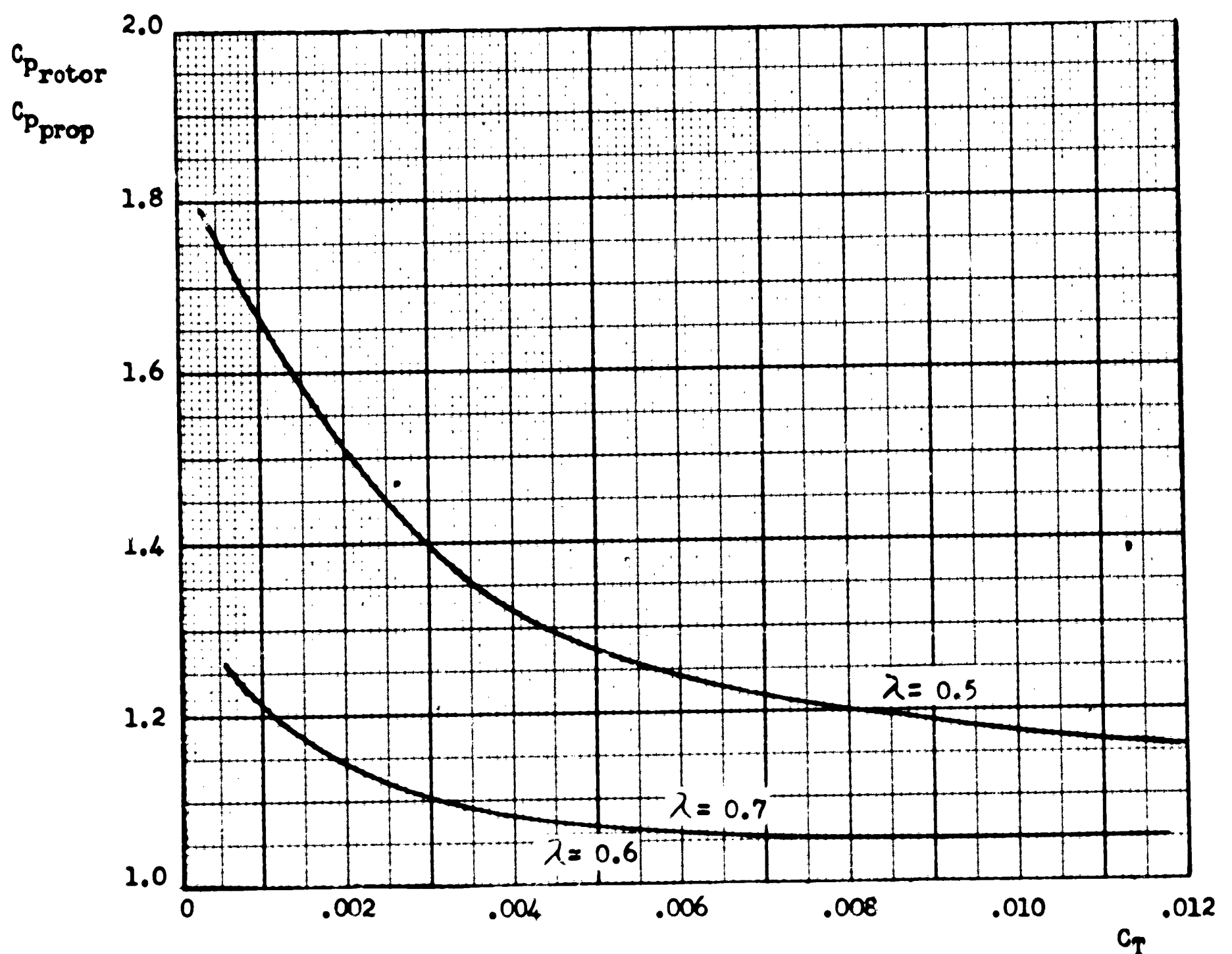
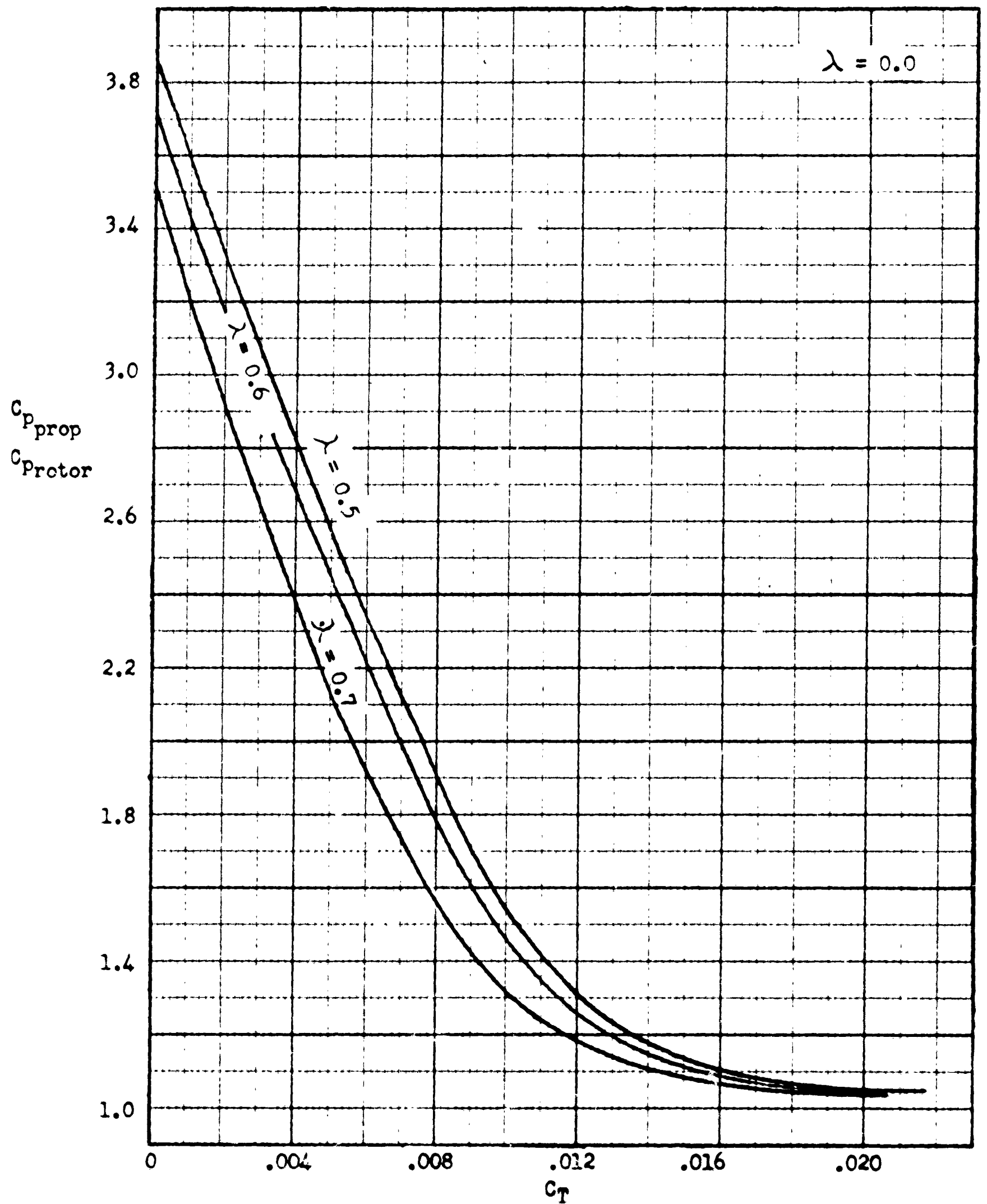


FIGURE 18

COMPARISON OF POWER REQUIRED BY AN OPTIMUM ROTOR AND  
AN OPTIMUM PROPELLER WITH BOTH PERFORMING AS A ROTOR



POWER REQUIRED BY OPTIMUM ROTOR AND OPTIMUM  
PROPELLER TO HOVER EXAMPLE TILT-WING TRANSPORT

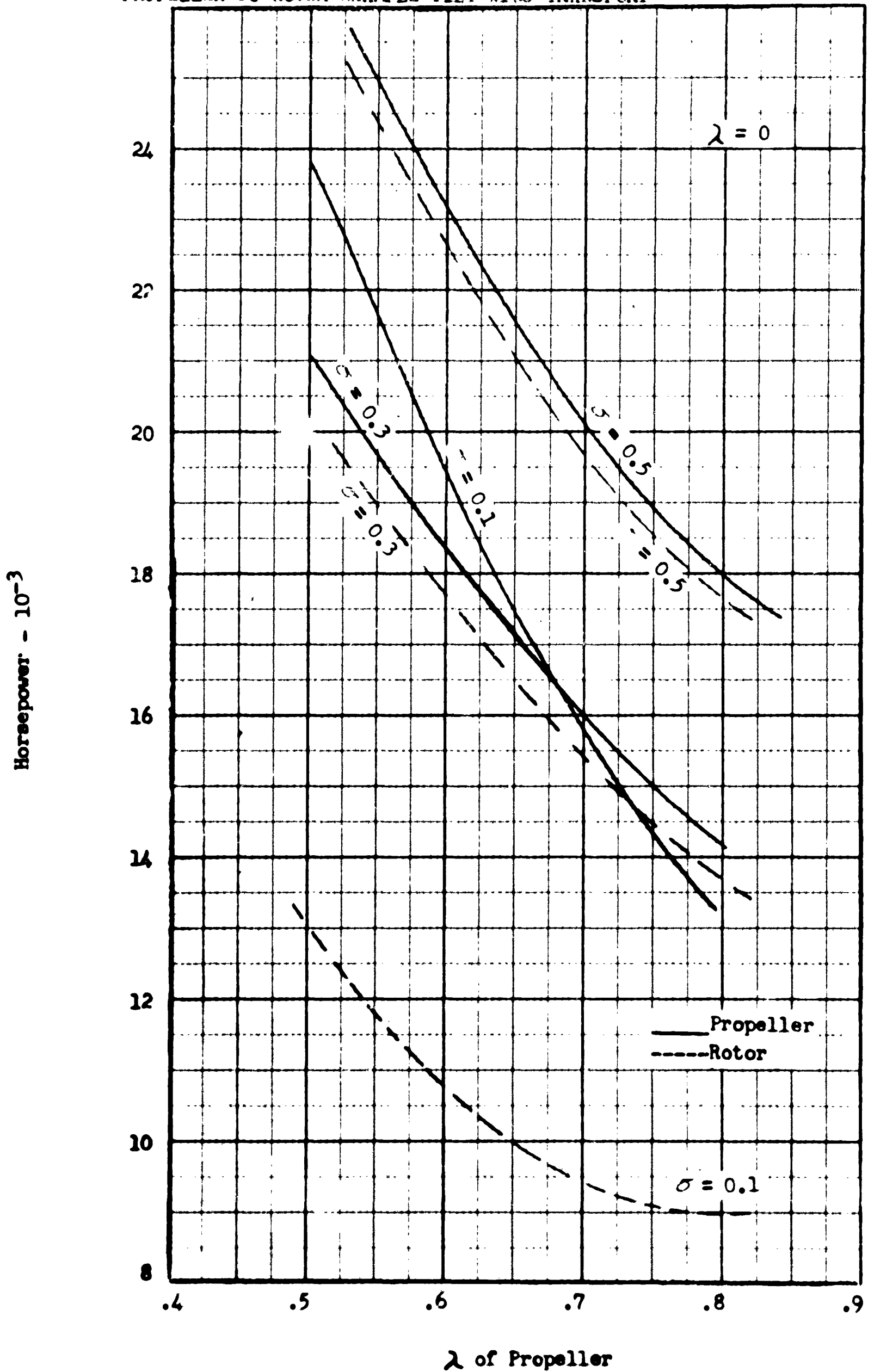


FIGURE 20

POWER REQUIRED BY OPTIMUM ROTOR AND OPTIMUM PROPELLER TO  
PROPEL THE EXAMPLE TILT-WING TRANSPORT IN FORWARD FLIGHT

